A QUALITATIVE MACHINE HEALTH ASSESSMENT BY RUNNING QUALITY INDEX

Olcay ÖNDER

İzmir Institute of Technology
July, 2008

A QUALITATIVE MACHINE HEALTH ASSESSMENT BY RUNNING QUALITY INDEX

A Thesis Submitted to
the Graduate School of Engineering and Sciences of
zmir Institute of Technology
in Partial Fulfillment of the Requirements for the Degree of

MASTER OF SCIENCE

In Mechanical Engineering

by
Olcay Önder

July 2008
ZM R

We approve the thesis of **Olcay ÖNDER**

Prof. Dr. Mustafa GÜDEN
Supervisor

Assistant Prof. Dr. Ebubekir ATAN
Committee Member

Assistant Prof. Dr. Cemalettin DÖNMEZ
Committee Member

15 JULY 2008

Date

Associate Prof. Dr. Metin TANO LU
Head of the Mechanical Engineering Department

Prof. Dr. Hasan BÖKE
Dean of the Graduate School of
Engineering and Sciences

ACKNOWLEDGMENTS

ABSTRACT

A QUALITATIVE MACHINE HEALTH ASSESSMENT BY RUNNING QUALITY INDEX

Mechanical components have limited life which is strongly related to the usage rate and operational conditions. Two parts could appear similar but actually not have the similar performances, because they had different usage rate, age, applied force and etc. during their life cycles. In this thesis, a new method that help to define the failure risk of mechanical components after customer utilization. The coding of Running Quality Index was performed in MATLAB program. The developed index summarizes all performance history of mechanical component/or part into a single number. A shaft test rig was designed to simulate force and number of cycle effects on the quality index. Tensile tests were conducted on St-37 steel samples exposed to varying forces, number of cycles and heat treatment to calculate Running Quality Index. The experimental results showed that increasing total number of cycles or repeated forces decreased the remaining life of samples. The developed quality index resulted in more risk penalty points for increasing number of cycles and repeated forces.

ÖZET

DE   KEN KAL TE ENDEKS NE GÖRE N CEL KSEL MAK NA SA LI I DE ERLEND RMES

Mekanik parçalar zamana ve kullanım artlarına ba lı olarak sınırlı bir ömre sahiptirler. Dı görünü ü aynı olan iki parçanın, farklı ya ta olmaları, ömürleri boyunca farklı yüklemeler görmeleri nedeniyle performansları aynı olmayacaktır. Bu çalı mada kullanıcının kullanımı sonucu ortaya çıkan, mekanik parçayı ba arısızlı a götüren risk unsurunun tanımlanmasında yardımcı olacak yeni bir metot önerilmi tir.

De i ken Kalite Endeksinin kodlaması Matlab programı ile yapılmı tır. Geli tirilmi olan endeks, mekanik parça veya bölümün tüm performans geçmi ini tek bir sayı ile özetlemektedir. Kalite endeksine kuvvet ve toplam devir etkilerini simule etmek amaci ile aft test düzene i dizayn edilmi tir. Birçok farklı yüklemeye, devir sayılarına ve sıcaklık etkilerine maruz kalan St-37 çelik malzemelere çekme deneyi uygulanarak De i ken Kalite Endeksi hesaplanmı tır.

Deneysel sonuçlar artan devir veya yük tekrarları ile örnek numunelerde kalan ya am süresinin azaldı ını göstermi tir. Geli tirilmi olan kalite endeksi daha çok tekrarlı yüke veya devire maruz kalan malzemeler için daha yüksek risk de erleri ile sonuçlanmı tır.

TABLE OF CONTENTS

LIST OF FIGURES

LIST OF TABLES

CHAPTER 1

INTRODUCTION

Risk is a concept that denotes a potential negative impact on an asset or some characteristic of value that may arise from some present process or future event. Risk can be assessed qualitatively or quantitatively. Qualitatively, the risk is considered to be proportional to the expected losses which can be caused by an event and the probability of this event (Çapan 2003). Measuring the engineering risk is often considered important but rather a difficult task. In engineering applications risk can be defined with the following general equation,

Risk = Probability of an Accident* Losses per Accident

As is expected, no equipment run with a nil failure rate; therefore, the optimization of the risk becomes an important issue in many occasions. The failure of a product may be due to any factor that causes lost of the functioning, for example the failure of one or more of components of a device (Pham 2006). Failures can easily result in life losses and economical hazards. Every year thousands of people injure or die as a result of mechanical failures. According to the CIA World Factbook published in July 2005, there were approximately 6,446,131,400 people on the planet and the annual death rate was approximately 8.78 per 1,000 people, corresponding to 56,597,034 human lost in every year. Approximately 30% died in traffic accidents or other industrial accidents, 50% died due to health problems and 20% died because of other reasons. In the failure of mechanical and/or structural components of devices, the risk of failure strongly depends on several criteria including fatigue, force repeat, temperature and failure distribution (Beer and Johnston Jr. 2003).

In this thesis, a new index for the failure risk of the mechanical components, after customer usage, has been developed. The Running Quality Index is different from the existent ones as being capable of separate the use from abuse. It gives more penalty points for the abuse use than normal use. The Running Quality Index include important factors such as force repeats, fatigue and temperature and it may also be further

extended by including more or less factors depending on the type of application. The code of the Running Quality Index has been developed by using Matlab.

CHAPTER 2

LITERATURE SURVEY

2.1. Fatigue

Materials fail under alternating loads, earlier than under static loads (Köksal 2005). Examples where the fatigue may occur include springs, turbine blades, airplane wings, bridges and bones. Failure of a material due to fatigue may be viewed in three stages as depicted in Figure 2.1. These stages are explained briefly below.

- Crack Initiation (stage I): Crack forms in this stage. The crack may be caused by surface scratches formed during handling or tooling of the material. Dislocations intersecting the surface as a result of previous cyclic loading or work hardening are also possible reasons for crack occurrence.

- Crack Propagation (stage II): The crack continues to grow during this stage as a result of continuously applied stresses. Small cracks become larger cracks eventually leading to failure.

- Failure (stage III): Failure occurs when the material that has not been affected by the crack cannot withstand the applied stress. This stage happens very quickly.
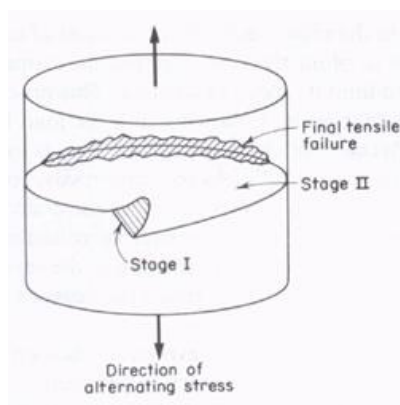
Figure 2.1. Location of the Three Steps In a Fatigue Fracture Under Axial Stress
(Source: Köksal 2005)

2.1.1. Early Works on Fatigue

Fatigue based damage theories developed before 1970's can be categorized into 4 groups:

1. Linear Damage Rules
2. The damage curve approach (DCA) & Double Linear Damage Rules
3. Fatigue damage theories based on crack growth
4. Work before 1970 attempted to improve the linear damage rule (LDR).

2.1.1.1. Linear Damage Rules

The first and simplest damage model is the Linear Damage Model (LDM). LDM was first developed by Palmgren in 1924 for the Swedish ball bearing industry. This rule is often referred to as Miner's rule. Miner applied the LDM to tension–tension axial fatigue data for aircraft skin material and demonstrated agreement between the predictions from the linear damage rule and his experimental results. Miner first represented the Palmgren linear damage concept as:

$$D = \sum r_i = \frac{\sum n_i}{N_{f\,i}} \tag{2.1}$$

where, D is a quantified damage accumulation parameter, n_i is the number of cycle experienced at a maximum stress, r_i is the cycle ratio corresponding to the ith load level, and N is the number of constant amplitude cycles. Typically, failure occurs when D reaches unity (Wahl 2001). Damage versus cycle ratio plot for this rule is a straight line as shown in Figure 2.2. (Vandewalle 2005).
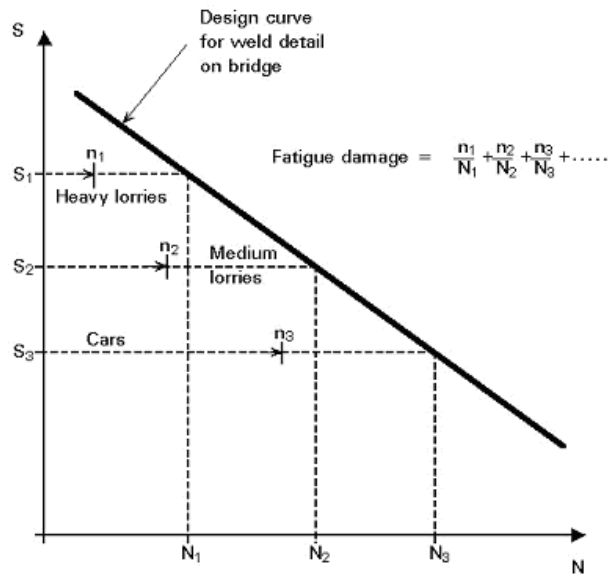
Figure 2.2. Cumulative Fatigue Damage for Loading at Different Stress Ranges

(Source: Vandewalle 2005)

2.1.1.2. Marco Starkey Theory

Marco and Starkey (Marco and Starkey 1954) proposed a non-linear load-dependent damage as,

$$D = \sum r_i^{xi} \tag{2.2}$$

where, x_i is a coefficient of ith loading. This rule allows to correctly account for the effects of different loading sequences. Only in some cases and for some materials, this law, and the other theories derived from it, has shown good agreement with experimental results. Because of that the method has a very limited application area.

2.1.1.3. Damage Theories Based On Endurance Limit Reduction

Another approach is to use the endurance limit reduction as a measurement of damage accumulation when multi-level load is applied. Komers and Bennett have investigated the effect of fatigue pre-stressing on endurance properties using a two-level step loading method (Gatts 1962). Komers and Bennett suggested that the reduction in

endurance strength could be used as a damage measure, but they did not correlate this damage parameter to the life fraction. This model firstly introduced by Henry (1954) in 1955 and later by Gatts LX. and Bluhm (Gatts 1961). Only few of these models take into account the effects due to the load interaction. In addition, the calculations are often too complex and accurate predictions are too difficult to be done.

2.1.1.4. Damage Curve Approach and Double Linear Damage Rule

2.1.1.4.1. Damage Curve Approach

The component's damage can be expressed in terms of an accumulation of the crack length toward a maximum acceptable crack length. This approach was developed to define the original Double Linear Damage Rule through a reliable physical basis. It is known that in fatigue the most important period is the fatigue crack growth where many complicated processes such as dislocation interactions and the multiple micro crack formation occur. Using this knowledge, Manson and Halford (Lee, et al. 2005) formulated the 'effective crack growth' model as:

$$a = a_0 + (a_f - a_0)r \tag{2.3}$$

where, a, a_0, and a_f are initial (r=0), instantaneous and final (r=1) crack lengths, respectively. A is a function of N in the form a = BN (B and   are material constants) In most cases, a_0=0 at the beginning so the equation becomes a function of r. Damage is then defined as:

$$D = \frac{a}{a_f} \tag{2.4}$$

For $a_0 = 0$, the equation becomes,

$$D = r^\alpha \tag{2.5}$$

It is obviously clear that this form is similar to Marco Starkey Theory.

2.1.1.4.2. Double Linear Damage Rule

Based on the observation that fatigue is at least a two-phase process (crack initiation and crack propagation) the models for the damage curves can be assumed to be bilinear. The double linear damage rule by Manson and Halford (Manson and Freche 1966) is recommended in engineering design for durability because of the tedious iteration process of the nonlinear damage theory. Manson (Franke and Dierkes 1999) divided the fatigue life into two phases to consider two load level effects as shown in Figure 2.3. The method uses the following relations:

$$\left(\frac{n_1}{N_1}\right)_k = 0.35 * \left(\frac{N_1}{N_2}\right)^{0.25} \tag{2.6}$$

$$\left(\frac{n_2}{N_2}\right)_k = 0.65 * \left(\frac{N_1}{N_2}\right)^{0.25} \tag{2.7}$$

Because of the nonlinear nature of damage and the accumulation of damage being modeled as a bilinear process, the two regions of damage are identified (Chena, et al. 2005). In Phase I, linear damage accumulation rule states that prior to reaching the knee point, the cycle ratios can be summed linearly and are independent of the loading sequence. When the sum of the cycle ratios reaches unity, Phase I damage is completed. After the total damage beyond knee point, the Phase II linear damage accumulation rule applies.
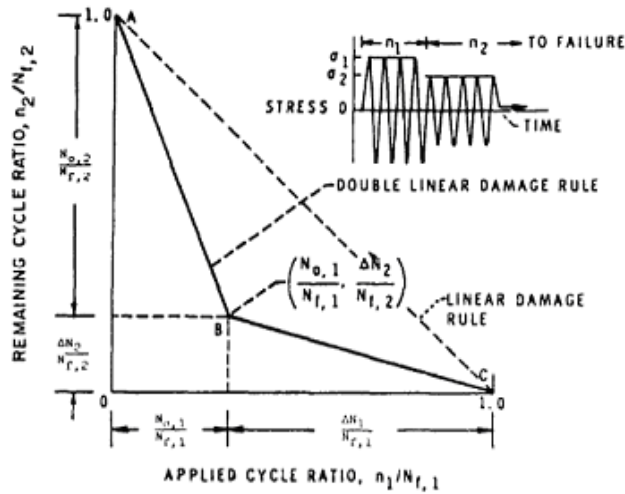
Figure 2.3. Double Linear Damage Curve

(Source: Chena, et al. 2005)

2.1.1.5. Damage Theories Using the Crack Growth Concept

The mechanisms that control fatigue crack growth, such as stress ratio, environment and other parameters have been widely studied, but are of continued concern to researchers. Another approach in cumulative fatigue damage analysis is the crack growth concept (Fonte, et al. 2007). The crack growth concepts developed in 1950's and 1960's have wide acceptance since cracks are directly related to damage. Before 1960's it was not possible to observe micro crack developments and only several macro crack theories developed. After the early 1970's, with the advanced technology, several new fatigue damage theories have been developed based on the micro crack growth concept. Most of these newer models better explain the physics of the damage than those developed before 1970's (Schlitz 1996).

2.1.1.5.1. Macro Fatigue Crack Growth Model

Fatigue limit can be explained from the physical perspective of the fatigue damage phenomenon under constant amplitude loading. Because of operating cyclic stresses, a micro crack will nucleate within a grain of material and grow to the size of about the order of a grain until a grain boundary barrier blocks its growth (Rama, et al.

2005). If the grain barrier is not strong enough, the micro crack will propagate to a macro crack and may lead to final failure.
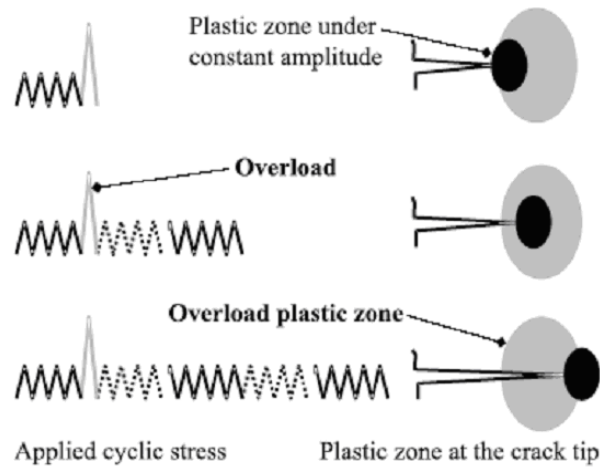
Figure 2.4. Impact of Fatigue Overload on Plastic Zone Side
(Source: Ray and Patankar 1999)

One of the popular macro fatigue crack growth retardation models is the Wheeler model. The residual stresses play an important role in the retardation caused by overload (Figure 2.4.) (Murthy and Palani 2003). Wheeler developed an expression to quantify the overload effects based on residual stress (Ray and Patankar 1999). To account for crack growth retardation, a retardation parameter, C_p is introduced. Retardation parameter (C_p) is a power function of the ratio of current plastic zone and overload plastic zone and shaping exponent as

$$\frac{da}{dN} = f(\Delta K) \tag{2.8}$$

$$a_n = a_0 + C_P f(\Delta K) \tag{2.9}$$

The retardation parameter is

$$C_P = \left(\frac{R_Y}{a_P - a}\right)^m \qquad \text{for } (a + R_Y) < a_P \tag{2.10}$$

$$C_P = 1 \qquad \text{for } (a + R_Y) > a_P \tag{2.11}$$

where, R_Y is the extent of current yield zone and $(a_P - a)$ is the distance from crack tip elastic-plastic interface and m is the shaping exponent. The limitation of this model is that the shaping exponent value is generally obtained with experimentations. Furthermore, this model does not predict acceleration caused by compressive overloads.

2.1.1.5.2. Short Crack Theory

Cyclically loaded components in structural applications often undergo to stress amplitude that is close to the fatigue limit of the material used. Under this kind of conditions, the phases of crack initiation and short crack propagation play an important role for the lifetime of the component. Miller investigated the relation between short cracks and their role for component lifetime. Miller and co-workers renamed the "crack initiation stage" and "phase I" as micro structurally short crack (MSC) growth and physically small crack (PSC) growth. In the MSC stage the plastic deformation is blocked by grain and phase boundaries until the critical stress level. Once the critical stress is reached, the plastic deformation and the crack can propagate into the next grain as shown in Figure 2.5. (Kunkler, et al. 2008). Based on experiments Miller (Zafosnik, et al. 2007) and co-workers described MSC and PSC as,

$$\text{Crack propagation rate} = A(\ )\ (d-a) \quad \text{for MSCs: } a_0 < a < a_1 \tag{2.12}$$

and

$$\text{Crack propagation rate} = B(\ )\ *a - C \quad \text{for PSCs: } a_1 < a < a_{final} \tag{2.13}$$

where, A,B, and are constants obtained by fitting experimental data., is the shear strain range, a_1 is the crack length corresponding to phase transition from MSC growth to PSC propagation, d is barrier size, and C is crack growth rate.

Mathematical forms of MSC and PSC are convenient for application to the analysis of fatigue. However the physics and validation of this theory needs more experimental work.
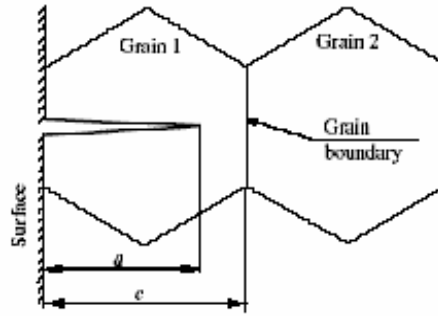
Figure 2.5. Formation of Short Crack Growth

(Source: Kunkler, et al. 2008)

2.1.2. Recent Theories

2.1.2.1. Subramanyan's and Hashin's Knee Point Approach

The knee-point approach was firstly introduced by Subramanyan (Krishnadev and Larouche 2008). Subramanyan calculated the damage as:

$$D_N = [\frac{n_n}{N_{n,f}}]^{(S_n - S_e)/(S_{critical} - S_e)}$$ (2.14)

where, $S_{critical}$ is critical stress and S_e is fatigue limit. Subramanyan's approach is not valid at stress levels near the fatigue limit of the material. Hashin expressed the knee point differently by using the fatigue life N_e at the fatigue limit S_e as,

$$D_N = [\frac{n_n}{N_{n,f}}]\log(\frac{N_{n,f}}{N_e})/\log(\frac{N_{critical}}{N_e})$$ (2.15)

Figure 2.6. shows a comparison between Subramanyan's and Hashin's approach. The former approach shows better agreements with the experiments.
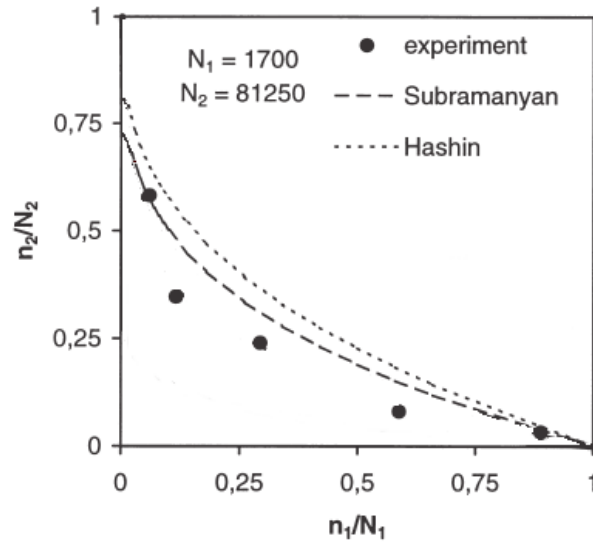
Figure 2.6. Comparison of Predicted Fatigue Behavior for Different Power Law Damage Rules with Experimental Data for SAE 4130 Steel (Source: Krishnadev and Larouche 2008)

2.1.2.2. Leipholz's Approach

Leipholz replaced the original S-N curve with a modified curve which took into account the load interaction effect. Leipholz's model is represented as,

$$\sum N = \frac{1}{\sum(\frac{\beta i}{Ni})}$$

(2.16)

where, N is the total accumulated life and β_i and N_i are frequency of cycle. In high-cycle fatigue situations, materials performance is generally characterized by an S-N curve, also known as a Wöhler curve (Figure 2.7.). The "S-N" means stress versus cycles to failure. In Figure 2.8., the S-N curve and the modified S-N curve by Leipholz are shown (Kohen 1999). At high loading levels, S-N curve is the same with the original curve but at low loading levels it deviates from the original curve (Kang, and Tan 2000). This method can provide accurate prediction of fatigue lifes under repeated block loading.
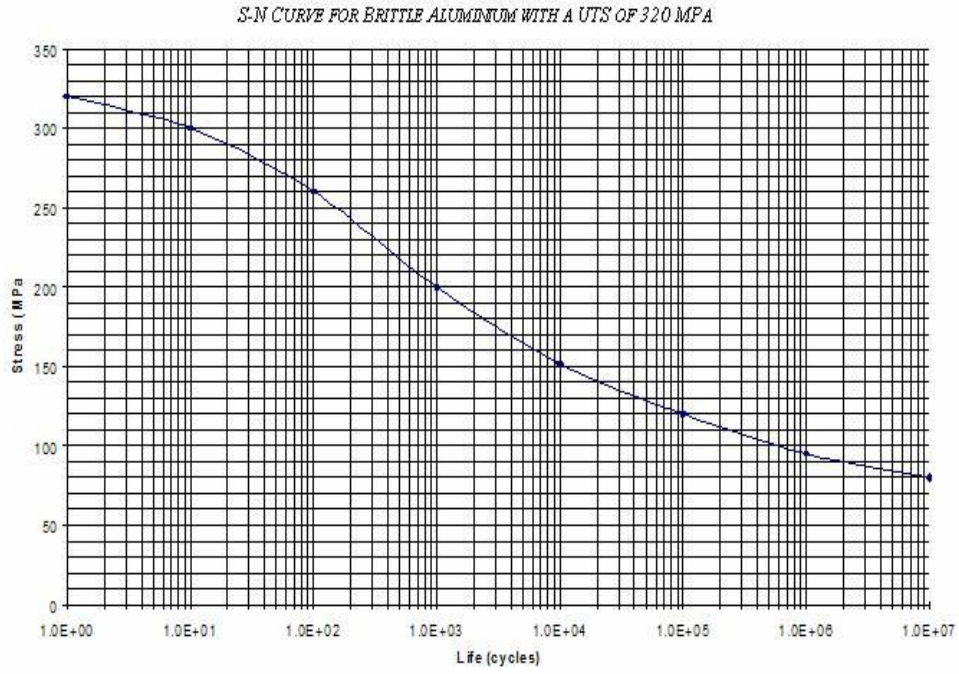
Figure 2.7. S-N Curve for Brittle Aluminum with a UTS of 320 Mpa

(Source: Kang and Tan 2000)
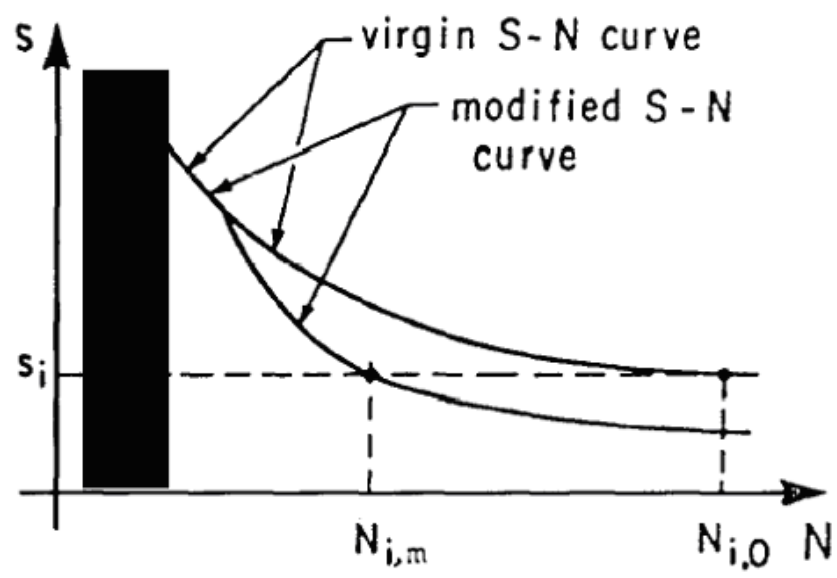
Figure 2.8. Schematic Representation of the Modified S-N Curve According to the Leipholz Approach. (Source: Kang.and Tan 2000)

2.1.2.3. Continuum Damage Mechanics Approaches (CDM)

CDM was first introduced by Kachanov (Liang.and Headrick 2006) and then developed by Lemaitre (Jadaan and Gyekenyesi 1996). It represents the damage in a continuum sense. The success of CDM application in the modeling of the creep damage process has encouraged many researchers to extend this approach to ductile plastic damage, creep-fatigue interaction, brittle fracture and fatigue damage. In addition to metallic materials, CDM can also be applied to composites (Desmorat, et al. 2006) and concrete (Jirasek and Grassl 2007). Three parameters important for a CDM model are the damage rate, damage indicator and failure criterion (Peerlings and Brekelmans 2006). The model relies on the assumption that damage decreases the effective cross-sectional area and increases the effective stress. The principle equation is given as

$$D = (1 - A - A_0) \tag{2.17}$$

CDM is very effective and easy to use but its predictions are found not matching with the experimental results as shown in Figure 2.9. Versions of this theory were also developed (Desmorat 2000).
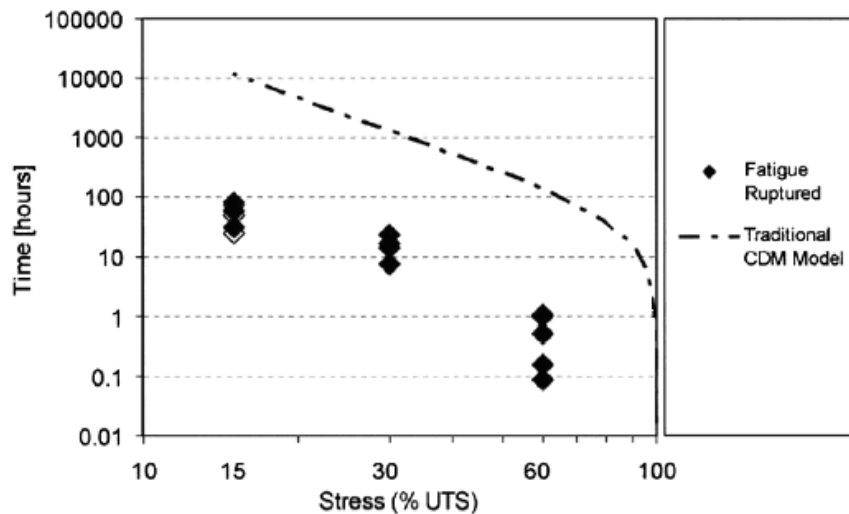
Figure 2.9. CDM Model versus Experimental Data

(Source: Desmorat 2000)

2.1.2.4. High Cycle and Low Cycle Fatigue Model

The fatigue behavior of materials is usually considered in two different regimes: low cycle regime and high cycle regime (Gerberich 1998). The boundary between low and high cycle fatigue cannot be defined easily based on a specific number of cycles. Nevertheless, 10^4 number of cycles are usually taken as the number of cycle which divides low and high cycle fatigue as shown in Figure 2.10. In high or low cycle models, the sole factor affecting fatigue life is the number cycles (Ashby and Jones 1998). Typically, the crack initiation period accounts for most of the fatigue life of a component made of steels, particularly in the high-cycle fatigue regime (i^{th} cycle > approximately 10^4 cycles). In the low-cycle fatigue regime (i^{th} < approximately 10^4 cycles), most of the fatigue life is spent on crack propagation (Stanzl and Mayer, 2001). Designing with respect to high or low cycle fatigue has their own advantages and disadvantages. The advantages and disadvantages are tabulated in Table 2.1. and 2.2., respectively.
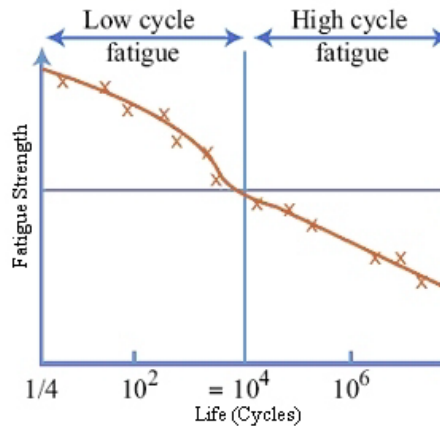
Figure 2.10. Low Cycle and High Cycle Fatigue Regime

(Source: Stanzl and Mayer 2001)

Table 2.1. Designing Advantages of HCF versus LCF

Designing Advantages Of HCF	Designing Advantages Of LCF
Empirical parameters for a lot of materials has been determined (ex:Fatigue Strengths)	More reliable than HCF
Easy to use for design applications	Widely used in industry

Table 2.2. Designing Disadvantages of HCF versus LCF

Designing Disadvantages Of HCF	Designing Disadvantages Of LCF
Cannot be used for Low cycle applications	Analysis depends on testing, strain data must be available
If loads are randomly HCF isn't reliable.	Analysis is more complicated that with HCF methods

2.1.2.5. Paris-Erdo an Law for Fatigue Crack Growth

Fatigue life prediction has a nearly 150 years of history. In the past, simple equations and laws were used to measure and predict fatigue crack growth. By the time technology develops and with the advent of mechanics, making prediction, or to at least understanding the mechanisms become easier with more complex and much efficient systems. The propagation ''speed'' was far from being constant in time: generally, the crack advance was larger for increasing stress amplitudes, but also for larger cracks, until the pioneering work of Paris (1961, 1963) who proposed a new law called Paris Law. Since then, many experiments have been conducted to understand completely the Paris law but today also a complete understanding of the law is absent (Kelly 2005). Paris Law is given by the following equation,

$$\frac{\Delta a}{\Delta N} = C * \Delta K^{n}$$

(2.18)

Where, C and n are material constants. Paris Law is widely accepted model in fatigue modeling because of its reliability in making of predictions. The relationships between crack size and crack resistance, crack driving force and crack size and crack growth rate and crack length of Paris Law are shown in Figure 2.11. It is noted in Figure 2.11. that after a critical crack size, the crack resistance becomes zero, leading to an increased crack growth rate. The life predictions using Paris Law gave also acceptable agreements with the experimental results as shown in Figure 2.12. for spot welded low carbon steel.
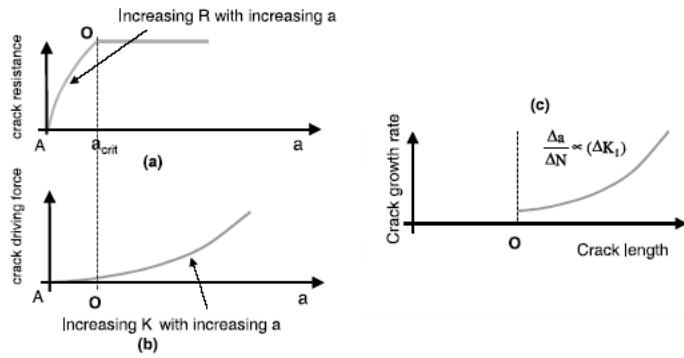
Figure 2.11. Paris Law and Crack Relationship

(Source: Kelly 2005)
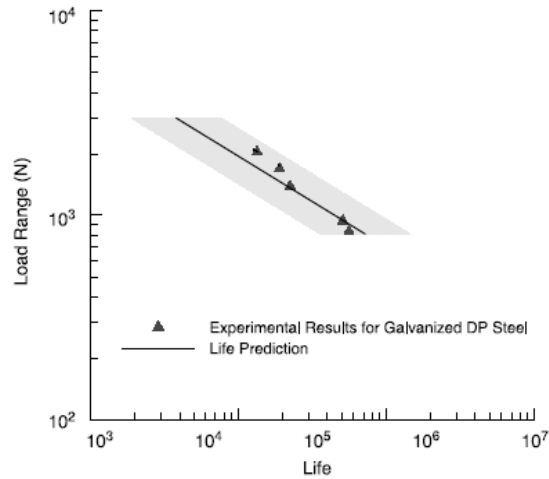
Figure 2.12. Predicted Fatigue Lives and Experimental Results for Spot Welds Made by Low Carbon Steels. (Source: Kelly 2005)

2.2. Stress Effects & Safety Factor

2.2.1. Safety Factor

The safety factor is used for the conditions over which the designer has no control: that is to account for the uncertainties involved in the design process. The most known uncertainties are as follows:

- Uncertainty regarding exact properties of material. For example, the yield strength can only be specified in between a range.
- Uncertainty regarding the size. The designer has to use the test data to design parts which are much smaller or larger. It is well known that a small part has more strength than a large one of same material.
- Uncertainty due to the effect of assembly operations like riveting, welding etc.
- Uncertainty due to effect of time on strength. Operating environments may cause a deterioration of strength, leading to premature and unpredictable failure of the part.
- Uncertainty in the nature and type of load applied.
- Assumptions and approximations made in the nature of surface conditions of the machine element.

The selection of the appropriate factor of safety to be used in design of components is strongly related with additional cost and weight and the benefit of increased safety or/and reliability. Generally an increased factor of safety results from a heavier component or a component made from a more exotic material or/and improved component design. An appropriate factor of safety is chosen based on several considerations.

2.2.1.1. How to Choose Safety Factor

Safety Factor = 1.25 - 1.5: Material properties and operating conditions are known in detail. Loads and resultant stresses and strains are known with a high degree of certainty. Low weight is important for the design.

Safety Factor = 1.5 – 2: Known materials with certification under reasonably constant environmental conditions, subjected to loads and stresses that can be determined using qualified design procedures.

Safety Factor = 2 – 2.5: Materials which will be operated in normal environments and subjected to loads and stresses that can be determined using checked calculations.

Safety Factor = 2.5 – 3: For less tried materials or for brittle materials under average conditions of environment, load and stress, safety factor must be selected between 2.5-3.

Safety Factor = 3 – 4: Safety factor of 3-4 selected for untried materials which will be used under average conditions of environment, load and stress. These large safety factors should also be used with better-known materials that are to be used in uncertain environments or subject to uncertain stresses.

The factor of safety is usually kept bigger, except in aerospace and automobile industries. In these the safety factors are kept low (about 1.15 - 1.25) because the costs associated with structural weight are so high. The low safety factor is the primary reason why aerospace parts and materials are subject to more stringent testing and quality control.

2.2.2. Stress Factor

The fracture of a material under different loading conditions is a complicated phenomenon that continues to attract the attention of physicists and engineers. Stress and strain are the quantities which used to compare the effects of a force on a material. A tensile force will stretch and, possibly, break the sample. However, the force needed to break a material will vary (depending on the cross sectional area of the sample). If the cross sectional area is bigger, the breaking force will be bigger. Stress-strain relationship gives the relation between unit stress and unit strain when plotted on a stress–strain diagram in which the ordinate represents unit stress and the abscissa represents unit strain. In the initial region the slope of the stress-strain curve gives the elastic modulus of the materials as shown in Figure 2.13.
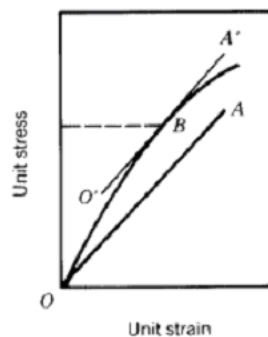
Figure 2.13. Stress-Strain Relationship Showing Determination of Apparent Elastic Limit (Source: Kohen 1999)

2.2.2.1. Surface Layer Stress Model

Information from the surface of a material usually plays an important role in damage analysis. Kramer (Mills, et al. 1996) introduced the concept of surface layer stress to characterize damage. During cycling, the specimen surface layer hardens due to a higher dislocation density than the interior and additional stress energy develops. Kramer defined this additional stress as the surface layer stress (σ_s) as,

$$D = \sum \left(\frac{\sigma_s}{\sigma_s{}^*} \right) \tag{2.19}$$

where, σ_{si} is the surface layer stress at i^{th} cycle and $\sigma_s{}^*$ is the critical stress level. The failure occurs when D = 1. The model could also be extended to corrosion-damage analysis, since corrosive attack promotes the surface layer stress (Yurci 1992).

2.2.2.2. Combined Stresses

Under certain circumstances of loading a body is subjected to a combination of tensile, compressive, and/or shear stresses. For example, a shaft that is simultaneously bent and twisted is subjected to combined stresses, namely, longitudinal tension and compression and shear. The expressions for the principal stresses in terms of the stresses along the x and y axes are given with following equations,

$$\sigma_1 = \frac{\sigma_x + \sigma_y}{2} + \sqrt{(\frac{\sigma_x - \sigma_y}{2})^2 + T_{XY}^2} \tag{2.20}$$

$$\sigma_2 = \frac{\sigma_x + \sigma_y}{2} - \sqrt{(\frac{\sigma_x - \sigma_y}{2})^2 + T_{XY}^2} \tag{2.21}$$

$$T_1 = \pm\sqrt{(\frac{\sigma_x - \sigma_y}{2})^2 + T_{XY}^2} \tag{2.22}$$

2.2.2.3. Maximum-Stress Theory (Rankine's Theory)

This theory is based on the assumption that failure will occur when the maximum value of the greatest principal stress reaches the value of the maximum stress (σ_{max}) at failure in the case of simple axial loading (Gdoutos 2005). Failure is then defined as,

$$\sigma_1 \text{ or } \sigma_2 = \sigma_{max} \tag{2.23}$$

2.2.2.4. Maximum-Strain Theory (Saint Venant)

This theory is based on the assumption that failure will occur when the maximum value of the greatest principal strain reaches the value of the maximum strain at failure in the case of simple axial loading. Failure is then defined as:

$$e_1 \text{ or } e_2 = e_{max} \tag{2.24}$$

2.2.2.5. Maximum-Shear Theory

This theory is based on the assumption that failure will occur when the maximum shear stress reaches the value of the maximum shear stress at failure in simple tension. Failure is then defined as:

$$T_1 = T_{max} \tag{2.25}$$

2.2.2.6. Distortion-Energy Theory (Hencky–Von Mises) (Shear Energy)

This theory is based on the assumption that failure will occur when the distortion energy corresponding to the maximum values of the stress components equals the distortion energy at failure for the maximum axial stress. Failure is then defined as:

$$\sigma_1^{\,2} - \sigma_1 * \sigma_2 + \sigma_2^{\,2} = \sigma_{max}^2 \tag{2.26}$$

2.2.2.7. Strain-Energy Theory

This theory is based on the assumption that failure will occur when the total strain energy of deformation per unit volume in the case of combined stress is equal to the strain energy per unit volume at failure in simple tension. Failure is then defined as:

$$\sigma_1^{\,2} - 2\sigma_1\sigma_2 + \sigma_2^{\,2} = \sigma_{max}^{\,2} \tag{2.27}$$

2.3. Failure Distributions

2.3.1. Basic Definitions

The Cumulative Probability Distribution Function (CDF): Probability of a component failing at a time of t (F(t)) is given as

$$F(t)=1\text{-}R(t) \tag{2.28}$$

The Reliability Function : Probability of a component surviving at a time of t is

$$R(t)=1\text{-}F(t) \tag{2.29}$$

Probability Density Function (PDF) : Probability of failure at an instant (a time period that is very small) is

$$f(t) = \frac{dF(t)}{dt} \tag{2.30}$$

Cumulative Failure Rate : Cumulative failure rate of a component at a time of t is,

$$\lambda_{cum}(t) = \frac{F(t)}{t} \tag{2.31}$$

Instantaneous Failure Rate (Hazard Rate): Probability of failure in unit time of a device that is still working is,

$$\lambda(t) = \frac{f(t)}{R(t)} = \frac{1}{R(t)} * \frac{dR(t)}{d(t)} \qquad (2.32)$$

Mean Time Between Failure & Mean Time To Failure: Mean time between failures (MTBF) is the mean (average) time between failures of a system, and is often attributed to the "useful life" of the device (not including 'infant mortality' or 'end of life' if the device is not repairable). Mathematically, the MTBF is the sum of the MTTF (mean time to failure) and MTTR (mean time to repair). MTTF is given as

$$MTTF = \frac{1}{\lambda} \qquad (2.33)$$

Mean time to failure is sometimes used instead of MTBF in cases where a system is replaced after a failure since MTBF denotes time between failures in a system which is repaired. Typical values of MTBF for increasing years are listed in Table 2.3.

Table 2.3. Mean time to failure between years (Constant Failure Rate)

(Source: Bloch 2006)

MTBF(Hours)	1-Year %Failure	2-Year %Failure	5-Year %Failure	10-Year %Failure
2.500.000	0.35	0.70	1.74	3.44
1.000.000	0.87	1.74	4.29	8.39
500.000	1.74	3.44	8.39	16.07
250.000	3.44	6.77	16.07	29.6
100.000	8.39	16.07	35.47	58.4
25.000	29.56	50.38	82.66	97.0

2.3.1.1. Bathtub Curve Model

In the 1950's, a group known as AGREE (Advisory Group for the Reliability of Electronic Equipment) discovered that the failure rate of electronic equipment had a pattern similar to the death rate of people in a closed system. Specifically, they noted that the failure rate of electronic components and systems follow the classical "bathtub" curve. This curve has mainly three phases (Figure 2.14.):

1. An "infant mortality" early life phase characterized by a decreasing failure rate (Phase 1). Failure occurrence during this period is not random in time. Parts fail with a high but decreasing rate.

2. A "useful life" period where components have a constant failure rate caused by randomly occurring defects and stresses (Phase 2).

3. A "wear out" period where the failure rate increases due to critical parts wearing out (Phase 3). As they wear out, it takes less stress to cause failure and the overall system failure rate increases, accordingly failures do not occur randomly in time.
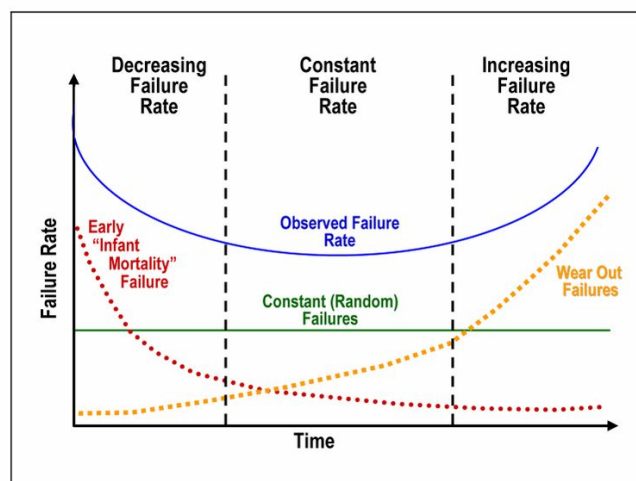
Figure 2.14. Bathtub Curve

(Source: Emerging Technologies for Design Solutions 2008)

Each region in bathtub can be modeled with a different reliability function as shown in Figure 2.15. The Weibull and log-normal functions are commonly used to model a changing failure rate in time while the exponential distribution is used to model

a constant failure rate in time (e.g., the steady-state portion of the bathtub curve). The Weibull is the most popular for modeling infant mortality while the log-normal function is often used in electronic component reliability to model wear-out.
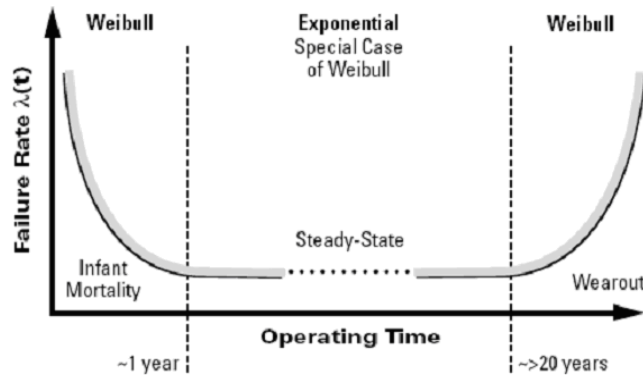
Figure 2.15. Bathtub Curve Distributions

(Source: World Nuclear Association 2007)

2.3.2. Main Distributions and Their Formulations

2.3.2.1. Weibull Distribution

The Weibull distribution is named after the Swedish physicist Waloddi Weibull, who modeled the distribution of the breaking strength of materials in 1939 and for a wide range of other application in 1951. The Weibull distribution is now one of the most widely used lifetime distributions in engineering. It is most commonly used in life data analysis. It is a general distribution that can be made to model a wide range of different life distributions by changing of the distribution parameters. Weibull introduced a probability distribution function of extreme value type into fatigue failure studies. Reliability analyses have been developed for metallic structures based on this distribution function. The Weibull distribution for a ball bearing is shown in Figure 2.16. The Weibull distribution function has also been used to model the fatigue life data of composites.
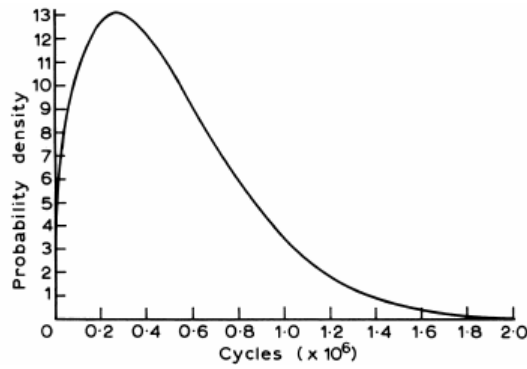
Figure 2.16. Weibull Function for a Ball Bearing

(Source: Pham 2006)

The pdf of Weibull Distribution is givens as

$$f(t) = \frac{\beta}{\lambda} * (\frac{t-L}{\lambda})^{\beta-1} * e^{-(\frac{t-L}{\lambda})^{\beta}}$$

(2.34)

The cumulative Weibull distribution F(t) is given as

$$F(t) = 1 - e^{-\lambda(t-L)^{\beta}}$$

(2.35)

where, is shape parameter, is the characteristic life (scale parameter) and L is the location parameter. If the shape parameter > 1, h(t) increases indicating symptomatic wear-out failures (Figure 2.17.). If <1, h(t) decreases. This would be typical for machinery components where run-in or initial self-accommodation takes place (Figure 2.17.). Mechanical shaft seals would be a typical example. When $= 1$, a special case of the Weibull distribution appears and failure rate becomes constant. If $= 2$, h(t) linearly increases with t; the resulting distribution is a special case of the Weibull function known as Rayleigh distribution.
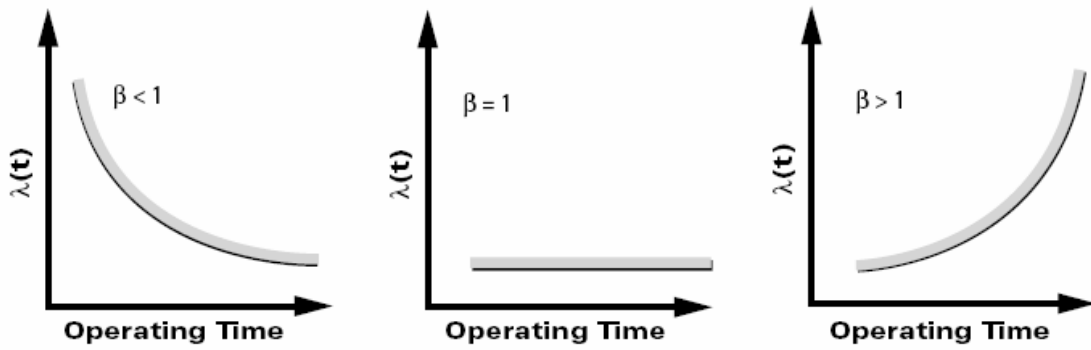
Figure 2.17. Weibull Distribution Functions

(Source: Pham 2006)

can be calculated graphically as:

$$\beta = \frac{\ln[\ln R(t_2)) - \ln[\ln R(t_1)]}{\ln(\frac{t_2}{t_1})}$$

(2.36)

The distribution function F(t) is given as,

$$F(t_i) = \frac{i}{(N+1)}$$

(2.37)

where, i :is sample number and N is total number of samples.

The reliability at t is defined as:

$$R(t) = \frac{(N+1-i)}{(N+1)}$$

(2.38)

$$R(t) = e^{-\lambda t^{\beta}}$$

(2.39)

$$\ln R(t) = -\lambda t^{\beta}$$

(2.40)

The Weibull probability density, distribution function and life function as function of t are shown in Figure 2.18. for various values of .
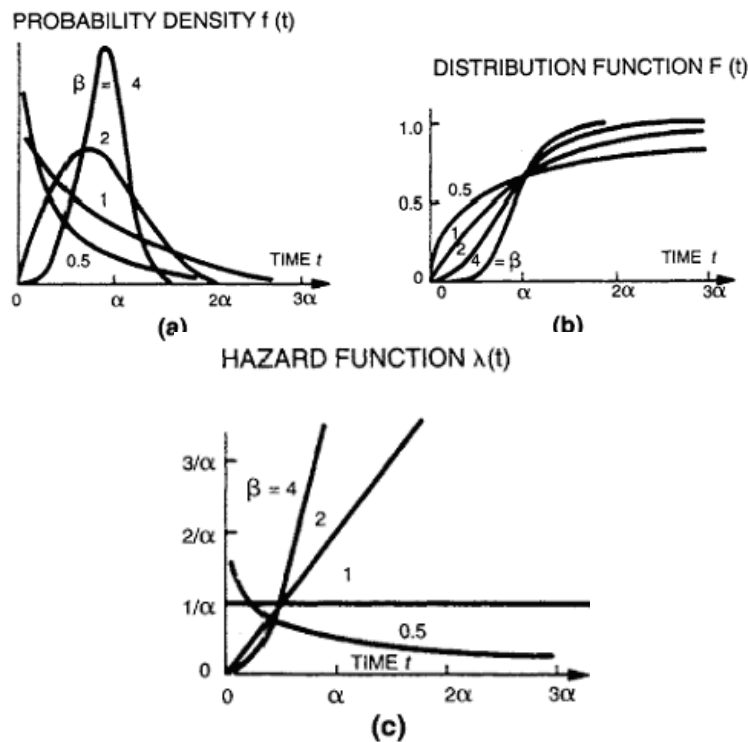
Figure 2.18. Plots of Weibull Distribution Functions. a) f(t) versus time. b) F(t) versus time. c) (t) versus time. (Source: Pham 2006)

The primary advantage of Weibull analysis is the ability to provide reasonably accurate failure analysis and failure forecasts for extremely small samples. Small samples allow cost effective component testing. Second advantage of Weibull analysis is that it provides a simple and useful graphical plot. The Weibull data plot is particularly informative. Another advantage of Weibull Distribution is its ability of modeling failure distributions. Analysis can be done in very short time with very good estimations. The main disadvantage of Weibull is that two-parameter Weibull distribution applies only in situations where the threshold parameter is known.

2.3.2.2. Normal Distribution

Normal Distribution (Figure 2.19.) discovered in 1733 by De Moivre as the limiting form of the binomial distribution (Bloch and Fred 2006). The normal distribution also called the Gaussian distribution is applicable to many fields. The importance of the normal distribution as a model of quantitative phenomena in the natural and behavioral sciences is due to the central limit theorem. Many physical measurements and physical phenomena such as noise can be approximated well by the normal distribution.
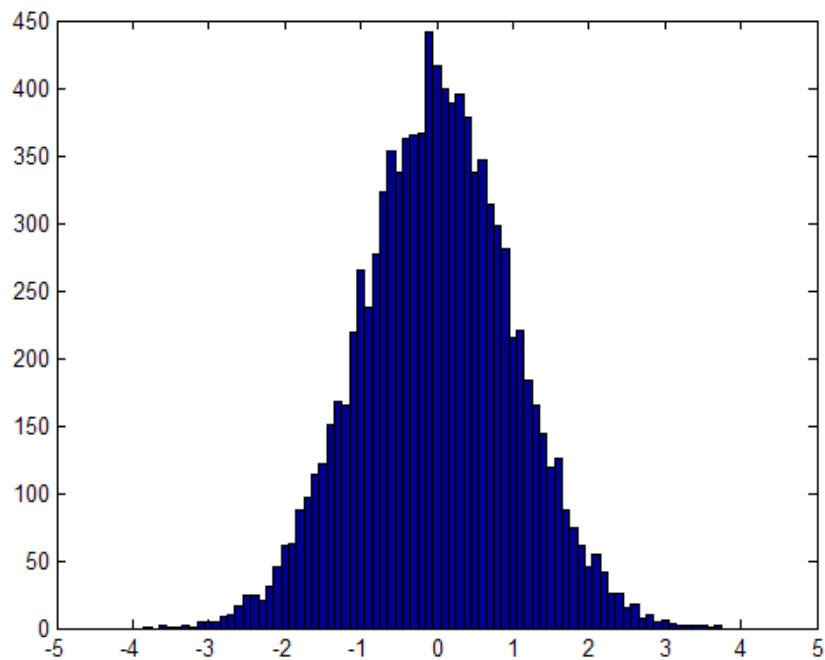
Figure 2.19. Normal Distribution

(Source: Mathnstuff 2007)

The probability density function (pdf) of the normal distribution is given as,

$$F(t) = \frac{1}{\sigma\sqrt{2\Pi}} e^{-\frac{1}{2}(\frac{t-\mu}{\sigma})^2}$$

(2.41)

The cumulative distribution function (cdf) of the normal distribution is,

$$R(t) = \int_{t}^{\infty} \frac{1}{\sigma\sqrt{2\Pi}} e^{-\frac{1}{2}(\frac{s-\mu}{\sigma})^2} ds \qquad (2.42)$$

where, μ is the location parameter and   is the scale parameter. The variation of the probability density function of the normal distribution for $\mu = 1.5$ as function of   is shown in Figure 2.20. When $\mu = 0$ and $= 1$, the normal distribution is called the standard normal distribution. Then the pdf becomes,

$$\Phi(z) = \frac{1}{\sqrt{2\Pi}} \exp(-\frac{z^2}{2}) \qquad (2.43)$$

The cdf of the standard normal distribution is

$$\Phi(z) = \int_{-\infty}^{z} \frac{1}{\sqrt{2\Pi}} \exp(-\frac{y^2}{2}) dy \qquad (2.44)$$
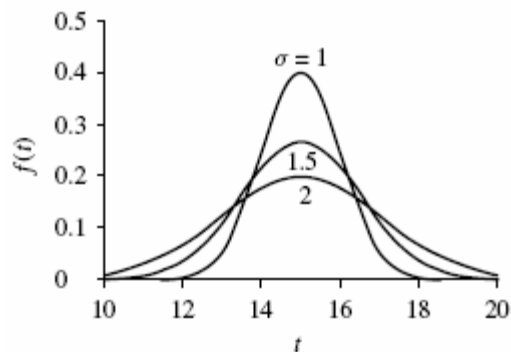
Figure 2.20. Normal Distribution for f(t) for $\mu = 1.5$.

(Source: Mathnstuff 2007)

The advantage of Normal Distribution is its simplicity and symmetry. The normal distribution is very useful in statistical analysis. It has further an important property frequently utilized in reliability design because of its proper results. It is also used in business administration. For example, modern portfolio theory commonly

assumes that the returns of a diversified asset portfolio follow a normal distribution. In human resource management, employee performance sometimes is considered to be normally distributed. Normal distribution method has also disadvantages. The distribution is limited in modeling life because it allows the random variable to be negative. It may be suitable for some product properties if the coefficient of variation (/μ) is small. It is used where failures are due to a wear process.

2.3.2.3. Exponential Distribution

The exponential distribution is a commonly used distribution in reliability engineering. It has wide acceptance in the reliability analysis of electronic systems. Mathematically, it is a simple distribution, which many times lead to its use in inappropriate situations. When events are purely random, the times between successive events are described by an exponential distribution. The failure rate for this distribution is , a constant, which is the main reason for this widely used distribution. At bathtub curve, the region of normal performance occurs at the area of constant failure rate. In this period (useful life) only random failures will occur. All parts and systems will have exponential distribution at this failure area. Since most parts and systems spend most of their lifetimes in this portion of the bathtub curve, this justifies frequent use of the exponential (when early failures or wear out is not a concern). The probability density function (pdf) of an exponential distribution has the form of

$$
\begin{aligned}
f(t) &= \lambda . e^{-\lambda x} \quad , x \geq 0 \\
f(t) &= 0 \quad\quad\quad , x < 0
\end{aligned}
$$

(2.45)

where, is a parameter of the distribution, often called the rate parameter. The distribution is supported on the interval [0,]. If a random variable X has this distribution, we write X~ Exponential ( ). The cumulative density function (cdf) is given as,

$$
F(x;\lambda) = \begin{cases} 1 - e^{-\lambda x} & , x \geq 0, \\ 0 & , x < 0. \end{cases}
$$

(2.46)

The mean of an exponentially distributed random variable X with rate parameter   is given as:

$$E\left[X\right] = \frac{1}{\lambda} \qquad (2.47)$$

Than the variance is defined as,

$$Var\left[X\right] = \frac{1}{\lambda^2} \qquad (2.48)$$

Plots of exponential distribution functions f(t), F(t) and   (t) are shown in Figure 2.21. In these graphs time is measured in units of 1/
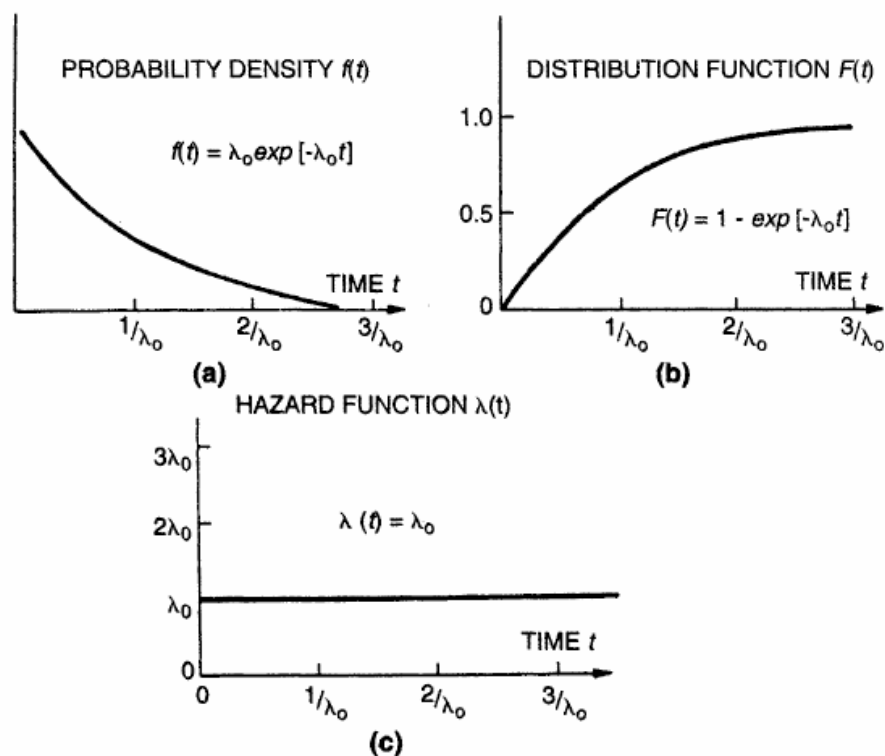
Figure 2.21. Plots of Exponential Distribution Functions. (a) f(t) versus time, (b) F(t) versus time,   (t) versus time. (Source: Pham 2006)

The exponential distribution can be used to construct basic probability models (such as assigning probabilities to various statements about a random variable) for the

behavior of a large number of phenomenon (for example, random variables of interest). It is commonly used to model the distribution of waiting times. Fragile materials and devices have a failure mechanism which is random overstressing at a roughly constant rate. Exponential distribution is applicable to systems that are repairable. Electronic equipments and brittles follow an exponential distribution during their useful life. The most important advantage of exponential distribution is its simplicity.

2.3.2.4. Where to Use Which Distribution

Table 2.4. shows few of the mechanical failure modes and the distribution suitable for them. Weibull Distribution is generally represents infant mortality or wear out mode. It is appropriate for accelerated life tests. Exponential Distribution represents constant rate process and describes only steady-state (useful life) portion of bathtub curve. Normal Distribution represent two-parameter bell-shaped curve model and used for process monitoring and control charts.

Table 2.4. Failure Modes and Their Probability Distributions
(Source: Bloch 2006)

Basic Machinery Components Failure Modes And Their Statistical Distributions			
	Probability Distributions		
Basic Failure Mode	Exponential	Normal	Weibull
1. Force /stress			
1.1. Deformation			X
1.2. Fracture	X		
1.3. Yielding	X		
2. Reactive Environment			
2.1. Corrosion		X	X
2.2. Rusting			X
2.3. Staining	X		
3. Temperature			
3.1. Creep		X	
4. Time Effects			
4.1. Fatigue			X
4.2. Erosion			X
4.3. Wear		X	X

In real life every product follows a different distribution. The Hazard Analysis Plot for the water pumps is given in Figure 2.22. This figure indicates that the water pumps have a median life of 9000 hours. At the first portion of the curve in Figure 2.22, the slope of the data is approximately 2.7 (=0.36) indicating a wear failure mode. At 1800 hours, the failure mode changes to a constant failure mode (=1); therefore the exponential distribution prevails in this region.
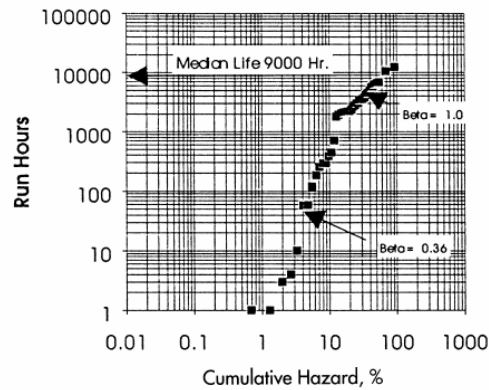
Figure 2.22. Exponential Distribution of a Water Pump

(Source: Bloch 2006)

Second example is given for the pump motors. The plot in Figure 2.23. indicates that the median life of the motors is approximately 13 000 hours. Up until that time, the failures are in "wear-in" or "infant mortality" mode. At about 13 000 hours,   becomes greater than 1, indicating that the motors begin to wear out.
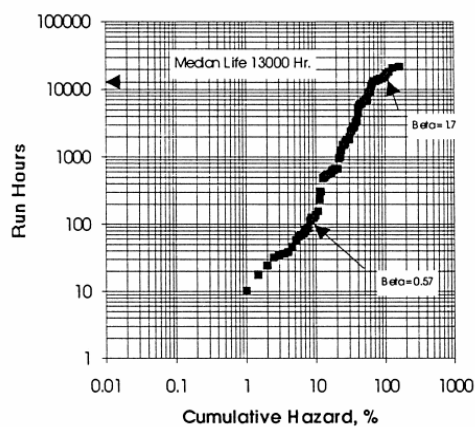
Figure 2.23. Motor Run Hours versus Cumulative Hazard

(Source: Bloch 2006)

Repair of equipments is an event often faced by the industry. Figure 2.24. helps us to make a decision. The plot has been generated by experimental results. For example the customer wants MTBF of 15 months with 97% percent reliability. We move vertically from 15 on the horizontal axis and intersect the reliability line of % 97 at a horizontal line corresponding to an allowable spare pump outage of 14 days.
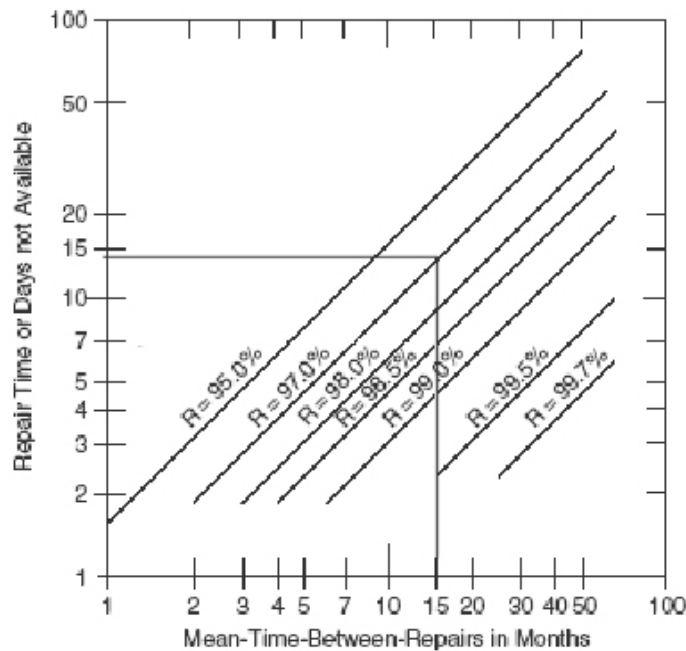
Figure 2.24. Pumps MTBF and Their Reliability

(Source: Bloch 2006)

2.3.2.5. Case Study: Application of RQI to Clutch Systems

Clutches are made of two basic components: the pressure plate and the disc (Figure 2.25.). In clutch life estimations, the following equations have widely acceptance,

$$Life = \frac{d}{W_p} \qquad (2.49)$$

and

$$W_p = \frac{k_0 * P * V_s * t}{A} \qquad (2.50)$$

where:

        d = Thickness

        k = Temperature influence factor

        P = Pressure between the clutch wear plates

        A = Clutch area

        t = Actuation Time in seconds

        V_s = Sliding Velocity in seconds

        W_p = Friction material wear per application

In clutch life estimation, there are several important parameters which dynamically change because of human factor. These parameters are sliding velocity in seconds (V_s) and actuation time in seconds (t). When the RQI will be used in clutch systems, it has to be based on clutch work time (t) and pedal angle ( ). These two parameters were selected because they change dynamically. The system was checked every 0.5 seconds. Reliable time for clutch working was selected as 3 seconds. If it will work more than 3 seconds, the situation brings risk and hazard (Figure 2.26.).
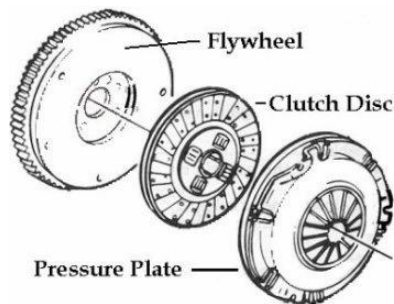
Figure 2.25. Clutch System

(Source: About Auto Repair 2007)
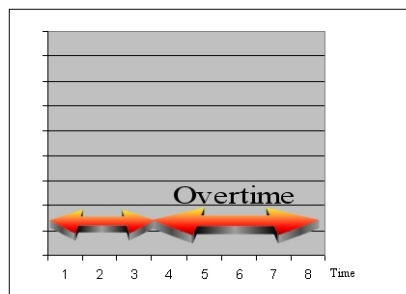
Figure 2.26. Overtime

For the pedal angle 30^0 is selected as reliable limit. If the angle is greater than 30^0 the risk will increase even the overtime has not occurred. The problem was simulated in MATLAB and angles for pedals was selected as 5,10,30,32,35,40,50,80,45 and 20. The variation of the pedal angle with time is shown in Figure 2.27. Running Quality index has the following formulation for clutch

RQI=(exp((Max reliable angle)/(Current Angle))*overtime*sliding velocity   (2.51)

Here for simplification the sliding velocity was taken constant and equal to 1. The risk density vs. time graph of the simulation is shown in Figure 2.28. The graph is plotted for 10 seconds and 20 results are taken in the simulation. The increase in the angle and the time causes an increase in risk density.
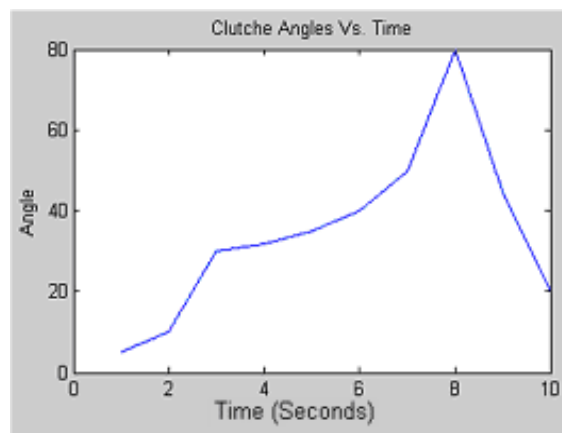
Figure 2.27. Pedal Angles with Respect to Time
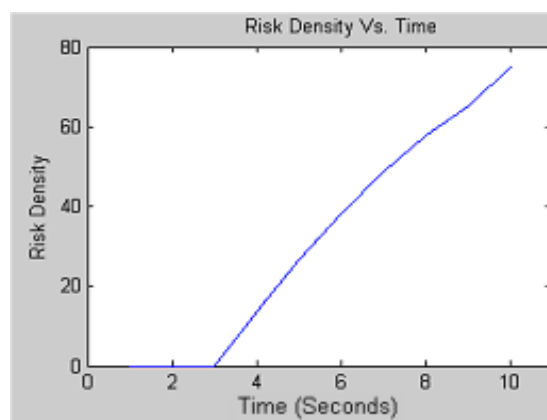
Figure 2.28. RQI Results of the Data in Figure 2.27.

2.4. Fracture

Fracture is the local separation of a body into two, or more, pieces under the action of stress (Figure 2.29.) and the fracture mechanics is a method for predicting failure of a structure containing a crack. The fracture mechanics uses methods of analytical solid mechanics to calculate the driving force on a crack. In modern materials science, fracture mechanics is an important tool in improving the mechanical performance of materials and components. It applies the physics of stress and strain, in particular the theories of elasticity and plasticity.
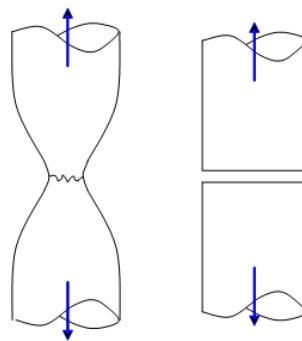
Figure 2.29. Demonstration of Fracture

(Source: Gdoutos 2005)

2.4.1. Fracture Mechanics

In many cases, the failure of engineering structures through fracture can be fatal as in the Tay Rail Bridge disaster (Figure 2.30.). The center section of the Tay Bridge collapsed during a storm on 28 December 1879, taking with it a train that was running on its track and more than 75 lives were lost (Martin and Iaian 2006). Investigators found that the cast iron columns supporting the longest spans of the bridge were of poor quality.
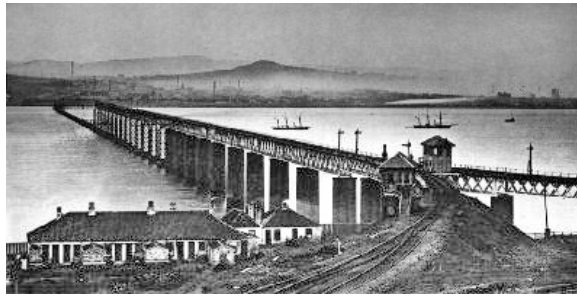
Figure 2.30. Tay Rail Bridge After Disaster

(Source: Martin and Iaian 2006)

One of the most widely known failure was that occurred in tankers and cargo ships that were built in the U.S.A in World War II. Shortly after they were built, several serious fractures appeared in few of them. The fractures were usually sudden and were accompanied by a loud noise. Most of the ships were less than three years old. In the period between November 1942 and December 1952 more than 200 ships experienced serious failures (Toth and Rossimanith 2003). Ten tankers and three ships broke completely in two. The ships experienced more failures in heavy seas than in calm seas and a number of failures took place at stresses that were well below the yield stress of the material. From these events, one can observe following general conclusions:

- Most fractures were mainly brittle in the sense that they were accompanied by very little plastic deformation, although the structures were made of materials with ductile behavior at ambient temperatures.

- Most brittle failures occurred in low temperatures.

- Usually, the nominal stress in the structure was well below the yield stress of the material at the moment of failure.

- Most failures originated from structural discontinuities including holes, notches, corners, etc.

- The origin of most failures was pre-existing defects and flaws, such as cracks accidentally introduced into the structure. In many cases the flaws that triggered fracture were clearly identified.

- The structures that were susceptible to brittle fracture were mostly made of high-strength materials which have low notch or crack toughness (ability of the material to resist loads in the presence of notches or cracks).

2.4.2. The History of Fracture Mechanics

Fracture Mechanics was invented during World War I by English aeronautical engineer, Alan Arnold Griffith (13 June 1893 – 13 Oct 1963), to explain the failure of brittle materials. Alan Arnold Griffith was an English engineer, who is best known for his work on stress and fracture in metals. At the time it was generally taken that the strength of a material was E/10, where E was the Young's modulus for that material. However it was well known that those materials would often fail at 1000 times less than this predicted value. Griffith discovered that there were many microscopic cracks in every material, and hypothesized that these cracks lowered the overall strength of the material. Griffith formulated his own theory of brittle fracture, using elastic strain energy concepts. The behavior of crack propagation of an elliptical nature by considering the energy involved has been described in his theory.

The equation basically states that when a crack is able to propagate enough to fracture a material, that the gain in the surface energy is equal to the loss of strain energy, and is supposed to be the primary equation to describe brittle fracture.

Inglis (1913), recognizing the destructive influence of cracks in brittle material, determined stresses around an elliptical stress-free hole and its extreme case of a fine straight crack, in a brittle, isotropic, homogeneous plate under tension using a mathematical approach. He showed that a pull applied to the ends of an elastic plate would produce tensile stresses at the tip of a crack that may exceed the elastic limit of the material and lead to the propagation of the crack. He found that the increase in the length of the crack exaggerates the stress even more such that the crack would continue to spread. Inglis showed that stress concentration was maximum at the tip of the long narrow hole and that the stress concentration factor depends on the shape of the hole and not its absolute size. He showed that the stress at the tip of the crack varies with the length and radius of curvature at the apices of the crack and is proportional to the square root of the length and inversely proportional to the radius of curvature of the crack.

Griffith (1921) was taken into account the effect of surface treatment on the strength of metallic machine parts as a first step. Early results by Komers indicated that the strength of polished specimens was about 45-50 percent higher than the strength of turned specimens. Furthermore, the strength was increased by decreasing the size of the scratches. In a research Griffith observed that tensile stresses appeared near the holes

according to their shape. These maximum stresses were independent of the size of the hole and depended only on the ratio of the axes of the elliptic hole. The maximum stress in the plate, $_{max}$ occurs at the end point of the major axis of the ellipse and is given by :

$$\sigma_{max} = \sigma(1 + \frac{2a}{b}) \approx 2\sigma\sqrt{\frac{a}{\rho}} \tag{2.52}$$

where, is the applied stress at infinity in a direction normal to the major axis of the hole, 2a and 2b are the lengths of the major and minor axes of the ellipse, respectively and ρ is the radius of curvature at the ends of the major axis of the ellipse. These results were in conflict with experiments. The strength of scratched plates depended on the size and not only on the shape of the scratch. In experiments of cracked circular tubes made of glass, Griffith (1921) observed that the maximum tensile stress in the tube was of the magnitude of 2372 MPa, while the tensile strength of glass was 172 MPa.

After these experiments Griffith developed the theorem of minimum potential energy to enable it to be applied to the critical moment at which rupture of the solid occurs. Griffith obtained the critical breaking stress of a cracked plate, and found it to be inversely proportional to the square root of the length of the crack. Thus he solved the problems of the Inglis solution (1921), that the strength of the plate is independent of the size of the crack. Griffith developed his theoretical predictions by making experiments on cracked spherical bulbs.

Consider a crack with area A. According to the law of conservation of energy, the change of the work,

$$\frac{dW}{dt} = \frac{dE}{dt} + \frac{dK}{dt} + \frac{d\Gamma}{dt} \tag{2.53}$$

where,

$\frac{dW}{dt}$: The work performed per unit time by the applied loads,

$\frac{dE}{dt}$ and $\frac{dK}{dt}$: The rates of change of the internal energy and kinetic energy of the body,

$\frac{d\Gamma}{dt}$: The energy per unit time spent in increasing the crack area.

Internal energy E can be represented as,

$$E = U^e + U^p \qquad (2.54)$$

where, U^e is the elastic strain energy and U^p is the plastic work. Since all changes with respect to time are caused by changes in crack size, then

$$\frac{d}{dt} = (\frac{dA}{dt})(\frac{d}{dA}); A \geq 0 \qquad (2.55)$$

If the applied loads are time dependent and the crack grows slowly the kinetic term K is negligible (Toth and Rossimanith 2003) and the Equation 2.55 becomes,

$$\frac{dW}{dA} = \frac{dU^e}{dA} + \frac{dU^p}{dA} + \frac{d\Gamma}{dA} \qquad (2.56)$$

Griffith (1924) recognized that during crack propagation surface energy is necessary to create new surface area. The total change in energy for crack propagation is,

$$G = \frac{dW}{dA} - \frac{dU^e}{dA} - \frac{dU^p}{dA} = \frac{d\Gamma}{dA} \qquad (2.57)$$

For an ideally brittle material plastic deformation is negligible and can be omitted from the equation 2.57 as

$$G = \frac{dW}{dA} - \frac{dU^e}{dA} = \frac{d\Gamma}{dA} \qquad (2.58)$$

During crack growth 2 new material surfaces formed (Griffith 1924), then equation 2.58 is written as,

$$G = \frac{dW}{dA} - \frac{dU^e}{dA} = \frac{d\Gamma}{dA} = 2\gamma \qquad (2.59)$$

The left handed side of the equation 2.59 represents the energy available for crack growth, and the right handed side represents the resistance of the material that must be overcome for crack growth. Two limiting cases: the "fixed grips" and " death loading " are usually used in practice.

In the fixed-grips loading configuration (Figure 2.31.), a specimen is stretched a fixed amount and then held rigidly by grips that remain stationary during crack propagation. The loading device is restrained by a very stiff load frame. Energy for driving the crack comes from the release of elastic strain energy within the stretched or bent specimen (Engelder and Mark 1995).
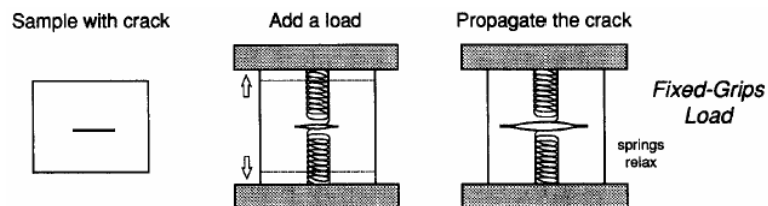
Figure 2.31. Fixed-grips Theory

(Source: Griffith 1924)

In the dead-load situation the applied loads on the surface of the solid are kept constant during crack growth (Figure 2.32.). Clapeyron's theorem of linear elastostatics states that the work performed by the constant applied loads is twice the increase of elastic strain energy. Therefore;

$$G = \left(\frac{dU^e}{dA} \right) = 2\gamma \qquad (2.60)$$
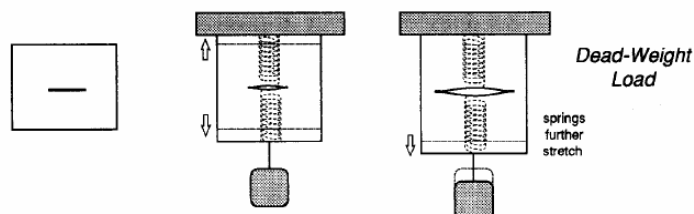
Figure 2.32. Dead-Weight Loading Theory

(Source: Griffith 1924)

Irwin (Ceriolo and Tomasso 1998) developed a relationship between crack length (a), surface energy connected with traction free crack surfaces (2) and applied stress as:

$$\sigma^2 = E * \left(\frac{2\gamma}{a\pi} \right) \qquad (2.61)$$

Griffith Theory predicted that compressive strength of a material is 8 times greater than its tensile strength; but this condition cannot be valid for any material. Later, the introduction of the line-crack (1957) made Irwin's approach more suitable than Griffith's crack for the need to consider the friction which develops between crack surfaces. Irwin provided the extension of Griffith theory to an arbitrary crack and proposed the criterion for a growth of this crack: the strain energy release rate (G) must be larger than the critical work (G_C), which is required to create a new unit crack area. This work resulted in a new materials property, fracture toughness (property which describes the ability of a material containing a crack to resist fracture), which is denoted K_{Ic}, and is now universally accepted as the defining property of fracture mechanics.

CHAPTER 3

DEVELOPMENT OF RUNNING QUALITY INDEX

3.1. Effects to Take Into Account

In developing the Running Quality Index the main goal is to create a new index to determine the risk levels of the component or parts which are operating. In order to determine risk, the effects which are the most important should be taken into consideration. Following the determination of the most important factors, the elimination phase started from less important factor to the most important factor. The elimination is inevitable: the control of every effect is not possible since a lot of computer memory and storage capacity are required. In this thesis, the total number load cycles and force repeat and temperature (heat treatment) are taken as the major effects on the Running Quality Index.

3.2. Determining Life Region

In order to develop a new quality index, the determination of which life region the index will be active is an important issue. There are 3 possible life regions in a bathtub curve in which the component life continues. These are; infant mortality, normal life and wear out regions. In the earlier region, the infant mortality mode, it is not possible to make accurate predictions because it is completely related with "bad luck". An example for that is the breakdown of a car within a thousand of cars produced; one cannot predict it before it happens. The second region where forms the flat part of the bathtub curve is considered as the useful life period where the failures occur because of usage, age, force, etc… In this region the failures are random but they are predictable in an extent. A 10-year old car obviously will have some problems. Running Quality Indexes are generally developed to work in the useful life period because most of mechanical components spend their life in this region. The righter part of the bathtub curve is called wear-out mode. In fact wear-out mode is interesting and valuable to take into account but it is an extreme case (like infant mortality mode). It is

completely related with chance. If the user is lucky than his/her product will continue its life after normal use conditions. The prediction about luck factor is not easy and is not accurate; therefore, the Running Quality Index does not make any estimation in the wear-out mode.

3.3. Selecting Appropriate Distribution

The next step in determining Running Quality Index is to define the appropriate distribution in the region. The Running Quality Index is mainly focused on the normal-use region. The user knows that after a certain year of use, the performance reduction will occur and if not repaired the component will fail. In the useful life region of a bathtub curve, the failures occur randomly; therefore an exponential distribution must be used as explained in section 2 of this thesis. The exponential distribution is accurate and simple for the fast Running Quality Index determination.

3.4. Modified Paris-Erdo an Law

In Paris-Erdo an equation, the total number of cycles has a significant effect on the crack development; therefore, the Risk is considered to be strongly related with the total number of cycles. The Paris Law is,

$$\frac{\Delta a}{\Delta N} = C \, \Delta K^n \tag{3.1}$$

The Paris Law dictates that the crack length has a strong dependency on N. If there is an increase in N, this will cause an increase in a. The increase in crack length will eventually cause the failure thus. Based on this, the Paris Law is modified for the determination of Running Quality Index. In the modified form of Paris Law, a is replaced with the increase in Running Quality Index (R). Second, ΔK^n is replaced with a stress term of $UTS\_Original / UTS\_Predicted$. This modification is made to define the probability of failure as functions of stress and heat treatment effects. Depending of the magnitude of the cycles and load repeats applied, the remaining part of the life will

change the UTS values. The manufacturer can define UTS_Final for a given set of conditions. Consider two steel shafts: one of them is at 1000^0C, while the other at room temperature. Predicted UTS value for the shaft working at room temperature will be higher than the UTS value of the shaft working at 1000^0C. Therefore, different risk levels may be obtained with respect to the temperature. For the last, the "C" term in Paris Equation is omitted since it is a constant. With respect to above mentioned modifications, the modified Paris Law is arranged as,

$$\Delta R = \left(\frac{\sigma_{UTS\_Original}}{\sigma_{UTS\_Predicted}} \right) * \Delta N \tag{3.2}$$

where, UTS_Original is the ultimate tensile strength when N=0 (determined experimentally by a single tension test at quasi-static strain rates) and UTS_Predicted is the material's predicted UTS. The Running Quality Index must be capable of taking into account every single effect coming from Equation 3.2; hence, the first part of the index can be calculated as the addition of all R variables:

$$Risk1 = \sum \left(\frac{\sigma_{UTS\_Original}}{\sigma_{UTS\_Predicted}} \right) * \Delta N \tag{3.3}$$

The above Risk1 equation takes total stress and number of cycles into account as the factors affecting the risk density.

3.5. A New Equation Based On Counting Every Single Force Effect and Critical Force Level

Designing mechanical products/components is usually done based on a coefficient which is known as "safety factor". The critical load is defined with respect to the safety factor as,

$$\frac{\sigma_{rupture}}{\sigma_{critical}} = SC \tag{3.4}$$

Where, $\sigma_{rupture}$ is the rupture stress and $\sigma_{critical}$ is the critical stress based on the safety factor. The rupture and critical stresses are written as,

$$\sigma_{rupture} = F_{rupture} / A \qquad (3.5)$$

$$\sigma_{critical} = F_{critical} / A \qquad (3.6)$$

In terms of load, Equation 3.4 is written as

$$\frac{F_{rupture}}{F_{critical}} = SC \qquad (3.7)$$

Based on the critical load the Running Quality Index is constructed with the following assumptions: every single force effect could be a reason for the failure even it does not pass the critical load and if a force exceeds critical force level, it will be more effective on the failure. Based on above assumptions, the probability of failure is

$$\frac{F}{F_{critical}} = P_{Risk\_of\_Failure} \qquad (3.8)$$

Where, F is the applied force at time of t, $F_{critical}$ is the critical force determined by the safety factor and $P_{Risk\_of\ Failure}$ is the probability of failure. This equation gives increased risk density punishment points when the F gets higher values. Using exponential distribution (McClave and Dietrich 1991) the following risk of failure equation is derived as:

$$\text{Every Single Force Related Risk of Failure} = z * e^{Prisk\_of\_failure} \qquad (3.9)$$

where, z is a parameter that counts for the number of times the material is used in the critical area. Equation 3.9 gives RQI which is the ability of defining risk density as a function of probability of risk of failure caused by every single force. In the development of RQI, the repeated force is taken as an important factor because many mechanical components are faced to repeated forces until the end of their useful life. If

the force exceeds the critical limit for the first time it may have not a very strong effect but when the exceeding occurs repeatedly, it becomes an important issue since every exceeding the critical load will have a more effect than that of the previous exceeding. In order to take into account this effect, a counter is placed into Running Quality Index codes which count the exceeding and give more risk penalty points for the next overload. By taking the summation of every single effect, it is possible to determine a cumulative effect as;

$$\text{Risk2=Force Related Risk of Failure} = \ z*e^{\text{Prisk\_of\_failure}} \qquad (3.10)$$

3.6. Running Quality Index

The Running Quality Index part is composed of two parts

$$RQI = Risk1 + Risk2 \qquad (3.11)$$

Where,

$$Risk1 = \sum \left(\frac{\sigma_{UTS\_Original}}{\sigma_{UTS\_Predicted}} \right) * \Delta N \qquad (3.3)$$

$$\text{Risk2} = \ z*e^{\text{Prisk\_of\_failure}} \qquad (3.10)$$

3.7. Demonstration of Running Quality Index

A force series formed by random is simulated (force_series =0.2*rand(100,1)) as shown in Figure 3.1. The following assumptions are made:

i)   Forces applied in 100 seconds.
ii)   The critical limit for applied force is 0.1 MPa.
iii)   Forces are repeated 100 times.
iv)   Total number of cycles is taken 100.

Since the random force series are used, the overloads occur randomly in useful life region. The calculated Risk2 is shown in Figure 3.2. It is noted in Figure 3.2 that the risk potential of all loadings are not the same even they have same values due to the repeat of the loadings over the critical limit. For an example after 20 seconds, the simulated product passes the critical load 6 times, while after 60 seconds 14 times. Therefore, more penalty points are given after 60 seconds.

Figure 3.1. Simulated Force Series

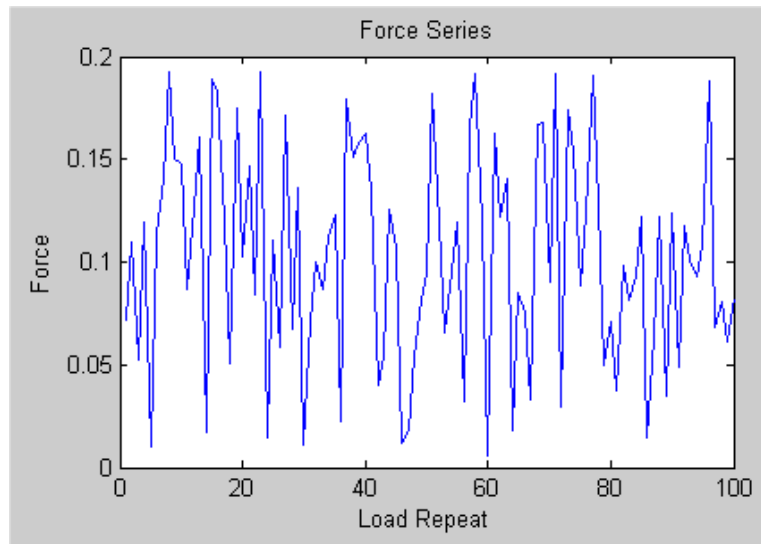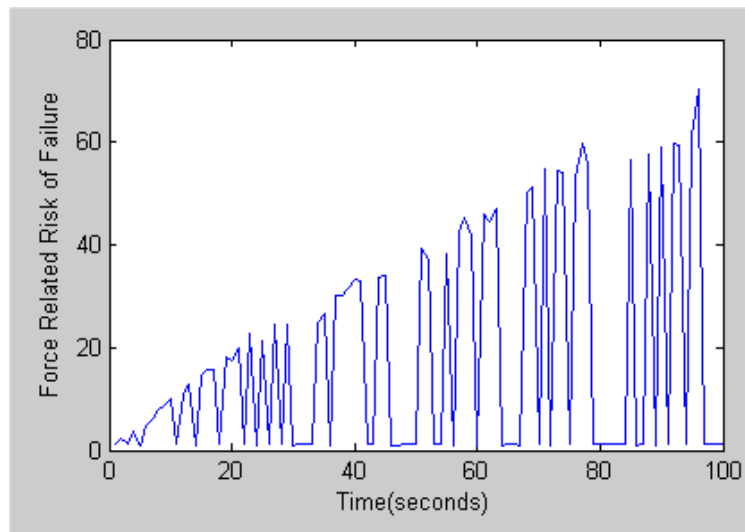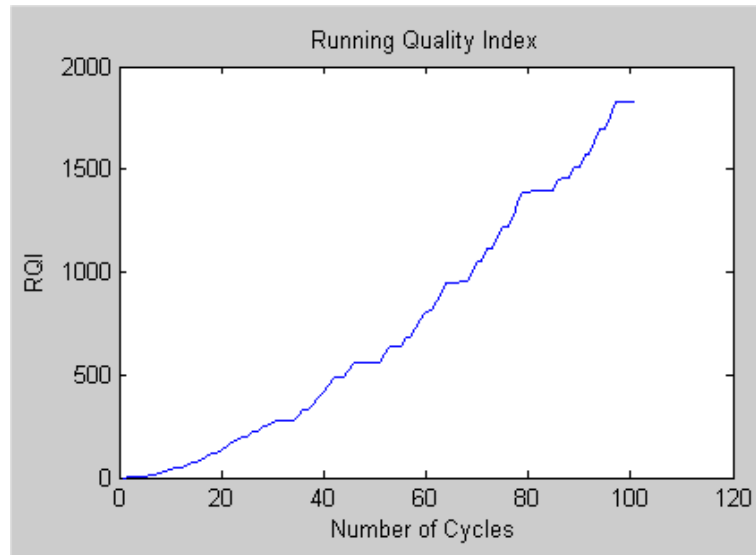Figure 3.2. Force Related Risk of Failure

Figure 3.3. Running Quality Index Results

The risk further increases with increasing the number of cycles as shown in Figure 3.3. The increase in Running Quality Index with increasing number of cycles is however not linear due to the force related risk. The increase in risk is more significant in areas where there is an overload as seen in Figure 3.3.

CHAPTER 4

EXPERIMENTAL

The purpose of experimental design is to validate Running Quality Index. The variables used for experimentation are total number of cycles, loading and temperature.

4.1. Experimental Design

A design is selected based on the experimental objective and the number of factors. Three different experimental designs and the number of factors are listed in Table 4.1. (Ryan 2006). If there are several factors but the primary goal of the experiment is to make a conclusion about one important factor and the question is that factor is very important or not, then comparative design must be used. In screening objective, the purpose of the experiment is to select or to screen out few important effects from the many less important ones. Response surface objective method (Haris 1976) is designed to give an idea of the shape of the response surface and it is used to find improved or optimal process setting and troubleshoot process problems and weak points. In this thesis, since the objective is to screen the important effects which are important and useful for developing a Running Quality Index, 2^3 Full Factorial Design was selected and used.

Table 4.1. Design Selection Guidelines.

(Source: Ryan 2006)

Design Selection			
Number of Factors	Comparative Objective	Screening Objective	Response Surface Objective
1	1-Factor Completely Randomized Design	-	-
2-4	Randomized Block Design	Full Factorial Design	Central Composite or Box-Behnken
5 or more	Randomized Block Design	Fractional Factorial or Plackett-Burman	Screen First To Reduce Number Of Factors

4.1.1. Full Factorial Design

Three dimensional cube as perspective drawing has been shown in Figure 4.1. Each cube dimension represents one factor in the experiment. With more factors, the cube becomes a hypercube. The design pattern is called 2^3 Factorial, three factors at two levels (high(+1) and low(-1)), eight design points on the corner points of the cube. Each design point presents experimental conditions at which one or more experiments must be run. In Figure 4.1., the factor x_2 has its low levels at the left side of the cube (four points) and it's high level at the right side of the cube. In the experimental design, x_1, x_2 and x_3 refer to temperature, force and total cycle, respectively. The tubular form of the design is shown in Table 4.2. The selected high and low values of design parameters are further listed in Table 4.3. The run order was used to eliminate experimental based errors (Table 4.4.). The Ultimate Tensile Strength values of the specimens were the response values.

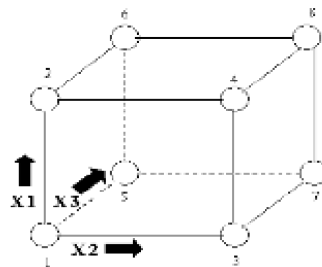Figure 4.1. Full-factorial Design

Table 4.2. Experimental Design Run Order and Factor Levels

Run	Force	Temperature	Total Cycle
1	-1	-1	-1
2	1	-1	-1
3	-1	1	-1
4	1	1	-1
5	-1	-1	1
6	1	-1	1
7	-1	1	1
8	1	1	1

Table 4.3. 2^3 Full Factorial Design

2^3 Full Factorial Design					
Study Type	Factorial		**Runs**	8	
Initial Design	Full factorial				
Factor	**Name**	**Low Actual**	**High Actual**		
A	Temperature	25^0C	800^0C	Levels	2
B	Total Cycle	268020	1072080	Levels	2
C	Force Repeat	50 times	100 times	Levels	2

Table 4.4. Run Order and Factors

Standard	Run Order	Factor1 (Temperature)	Factor 2 (Total Cycle)	Factor 3 (Force Repeat)
4	1	800	1072080	50
7	2	25	1072080	100
8	3	800	1072080	100
5	4	25	268020	100
1	5	25	268020	50
3	6	25	1072080	50
6	7	800	268020	100
2	8	800	268020	50

4.2. Description of the Test Rig

Figure 4.2. shows the used test bench set-up. The rig contains a shaft which was supported by two roller bearings (Figure 4.3.). The MSB roller bearing had a diameter of 15 mm. The shaft was connected to the AC motor (Figure 4.4.) with a strap. The loading of the shaft was done by a hydraulic piston unit (Figure 4.5.). The properties of the hydraulic power were as follows: Motor Power: 380 Volt / 50 Hertz / 1.1 Kilowatts Oil Tank: 24 lt, Working Pressure: 0-100bar, Cylinder: - Closed Length: 600 mm, Open Length: 1000mm, Stroke: 400mm.

A control panel was designed to operate hydraulic piston and AC motor. A digital tachometer was used to measure the rpm of the shaft. The shaft was rotated at a

constant rpm, 1490. The control panel of the system was placed at a safe distance from the setup. Two security switches (Figure 4.6.), one for automation system and motor, one for hydraulic power unit, were installed on the control panel that allows immediate shut-down. An automation system was installed on control panel to control the hydraulic unit. Automation system had two selections: automatic control of hydraulic system which allowed to define exact "on - off" times of hydraulic unit and manual control of hydraulic system which allowed to control the system manually for calibration.

Total 10 samples were tested: 5 of these samples were heat-treated at 800^0C for 30 minutes before testing. In the test rig, total cycle and force repeats varied in the range of 268,020-1,072,080 total cycle and 50-100 times to determine different life properties. The critical loading level was selected as 1.1MPa for non-heat treated samples and 1 MPa for heat-treated samples.

Figure 4.2. Test Rig

Figure 4.3. Roller Bearing

Figure 4.4. Pump Motor

Figure 4.5. Hydraulic Power Unit

Figure 4.6. Control Panel

4.3. Material

St 37 steel was tested for the experiments. The material properties and chemical composition of the steel is tabulated in Table 4.5. The tension test samples dimension (Table 4.6.) was in accord with ICS 77.040.10 TS 138 standard. The tensile test specimen picture is shown in Figure 4.7.

Table 4.5. St 37 Material Properties

ST 37 MATERIAL PROPERTIES		
Chemical Properties (%)		
C	Mn	Si
0.08	1.20	0.50
Mechanical Properties (%)		
Tension Strength (N/mm^2)		Yield Strength (N/mm^2) min W<16
600-700		235

Table 4.6. Test Samples Dimensions

Test Samples Dimensions	
G	55.0 ± 0.5 mm.
W	7 ± 0.10 mm.
R	5 mm.
L	150 mm.
A	65 mm.
B	35 mm.
C	14.9 mm.

Figure 4.7. Test Sample

4.4. Tension Testing

   After applying the determined variables on the tensile test samples, tension tests were performed using a displacement controlled SHIMADZU AG-I universal tension-compression test machine (Figure 4.8.). Tests were performed at a cross-head speed of 3mm min^{-1}. Yield stress, ultimate tensile stress and failure strain values were determined from the stress strain curves. A demonstration of testing system is given in Figure 4.9.
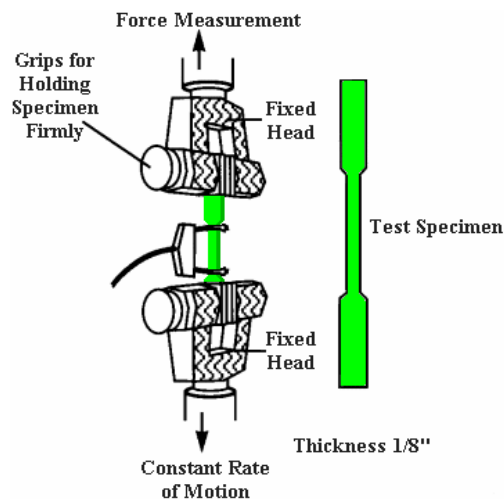

Figure 4.8. Tensile Test Machine

Figure 4.9. Tensile Test Demonstration

CHAPTER 5

RESULTS AND DISCUSSION

5.1 Tensile Test Results

Load-displacement curves of the 8 samples tested are shown sequentially in Figure 5.1.-5.8. UTS values of the samples tested are further listed in Table 5.1. The load-displacement curves indicate that samples which exposed to less number of cycles or load have higher Ultimate Tensile Strength than the samples exposed to higher number of to cycle or load.
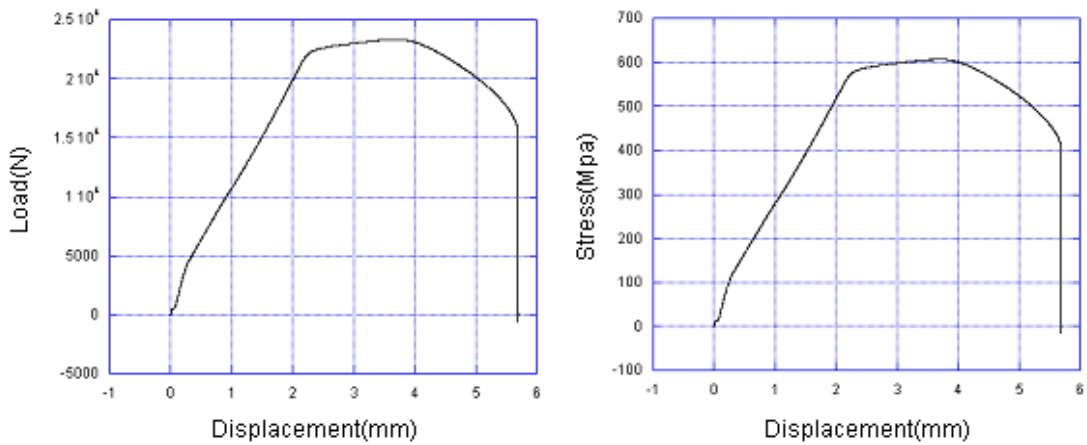

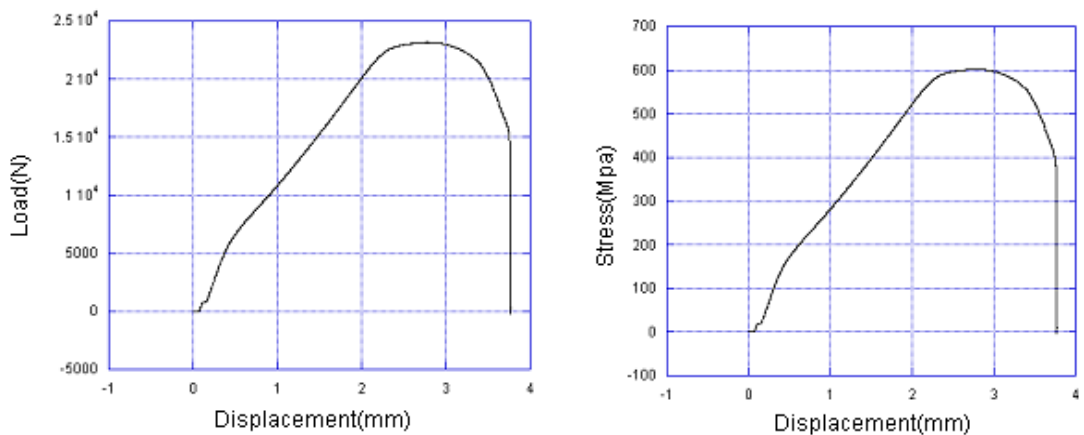Figure 5.1. Tensile Test Results for Sample 1

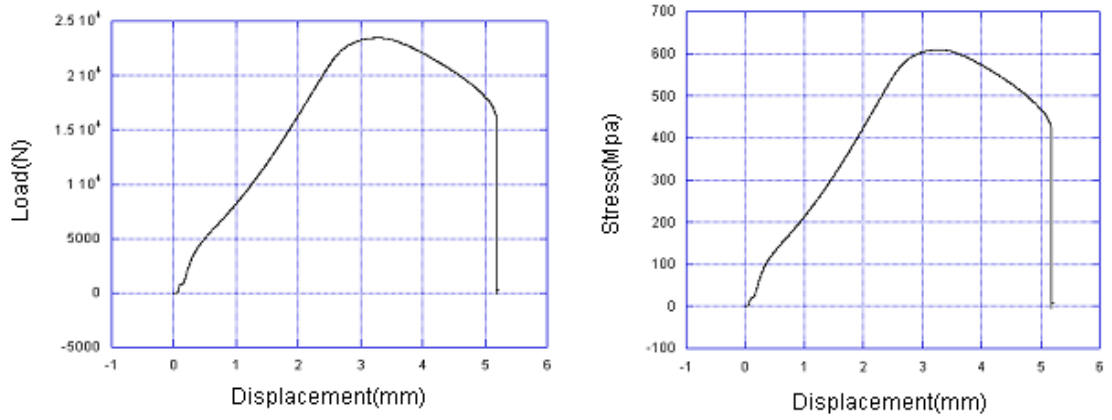

Figure 5.2. Tensile Test Results for Sample 2

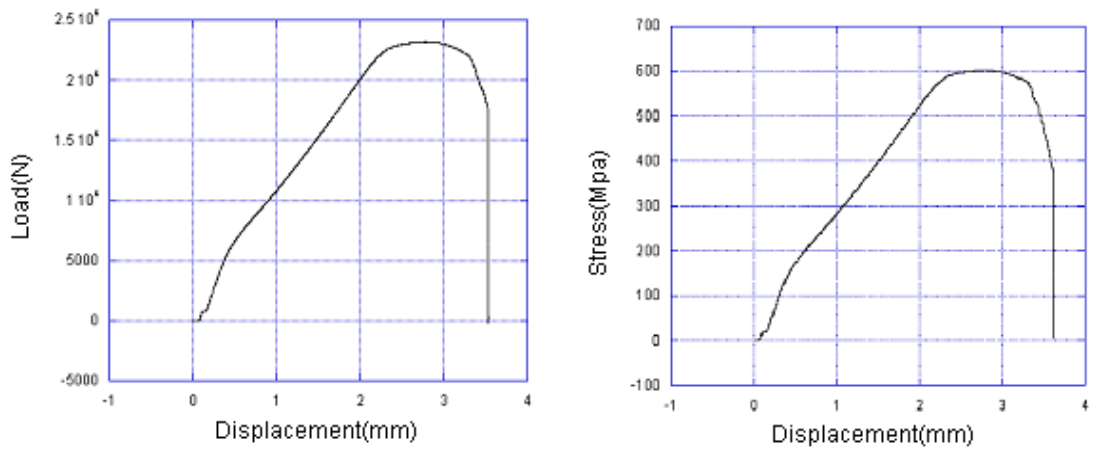Figure 5.3. Tensile Test Results for Sample 3

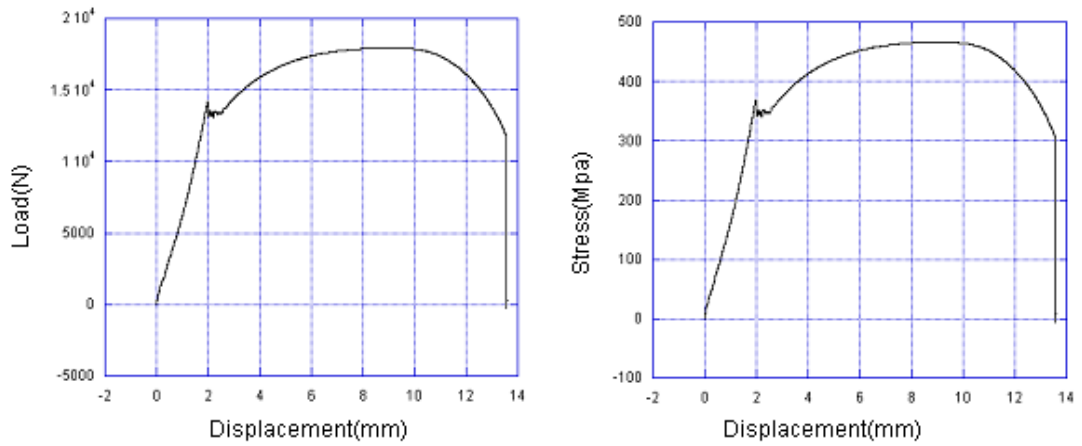Figure 5.4. Tensile Test Results for Sample 4

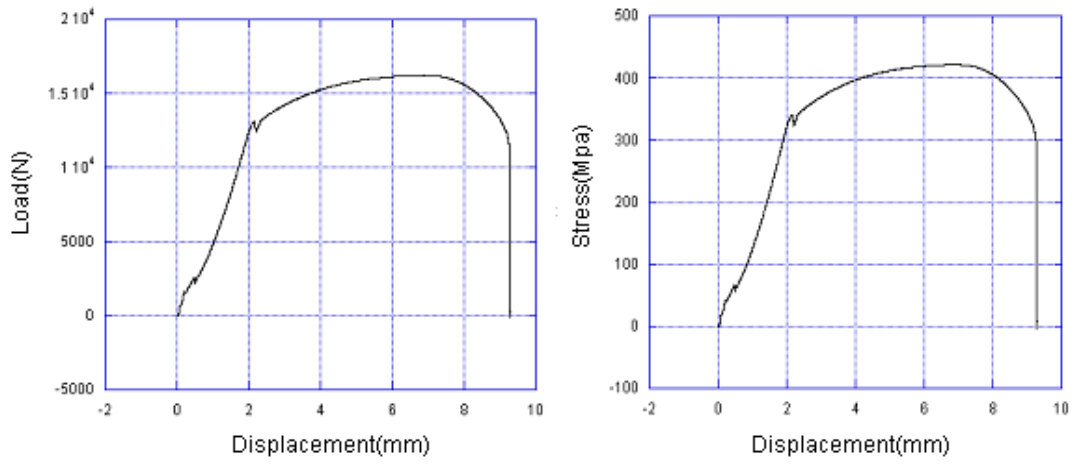Figure 5.5. Tensile Test Results for Sample 5

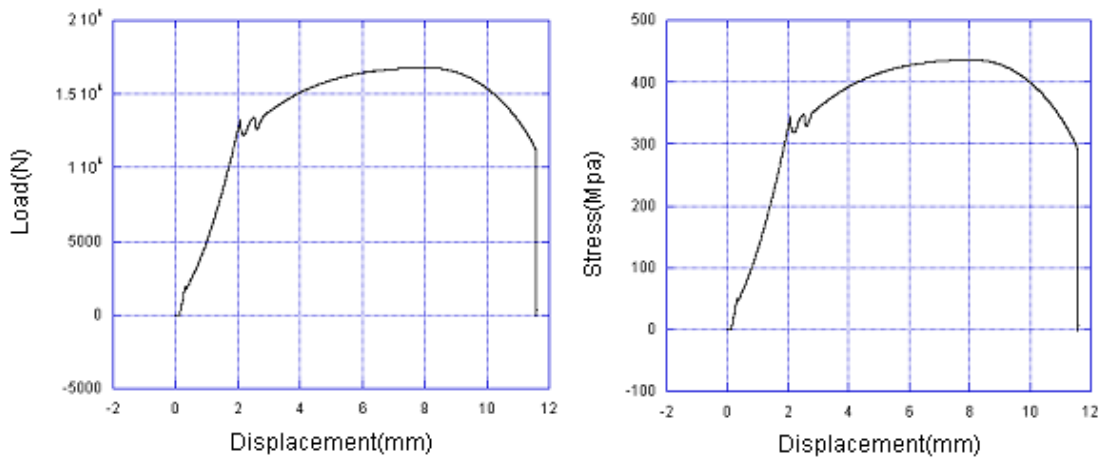Figure 5.6. Tensile Test Results for Sample 6
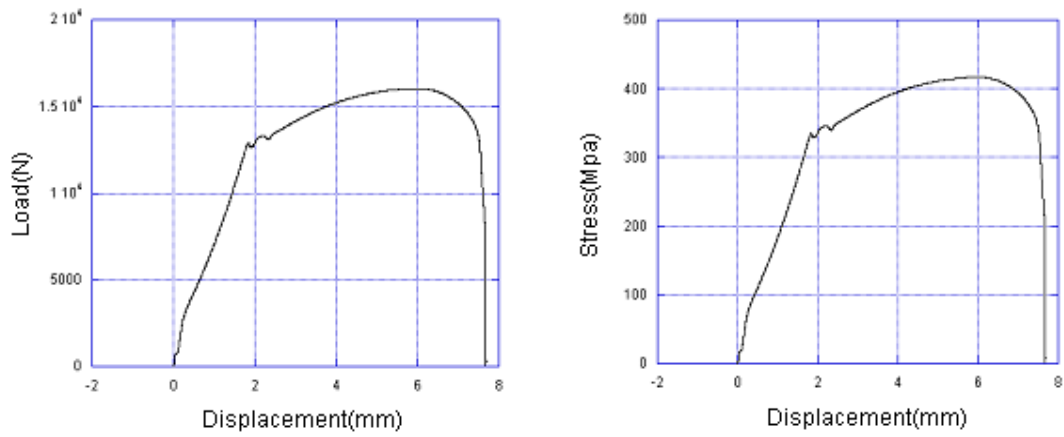

Figure 5.7. Tensile Test Results for Sample 7

Figure 5.8. Tensile Test Results for Sample 8

Table 5.1. UTS Values of Samples

Sample Number:	Original UTS Value (MPa)	Predicted UTS Values (MPa)
1		549.081
2		542.718
3	633.79	545.625
4		541.674
5		409.914
6		379.431
7	466.47	392.679
8		375.138

5.2. Running Quality Index Results

Running Quality Index is defined as:

$$RQI = \sum \left(\frac{\sigma_{UTS\_Original}}{\sigma_{UTS\_Predicted}} \right) * \Delta N + \sum z * e^{\Pr isk\_of\_failure} \tag{3.10}$$

The simulation results of 8 samples tested are shown sequentially in Figures 5.9.-5.16. It was observed that, the increase of load repeats or number of cycles has an important effect on the UTS values as seen in Figures 5.9.-5.16. Running Quality Index does not increase linearly and it gives different risk points at different loadings. For example, in Figure 5.12., the load is less than 1.1MPa (critical force level) and Running Quality Index gives less penalty points, while loads exceeding 1.1MPa give more penalty points. Running Quality Index is also capable of counting how many times there is exceeding the critical load and gives more penalty points for the second point of critical load exceeding. Running Quality Index has successfully calculated risk density for different samples with different conditions. The decrease in UTS values increases the failure probability. Table 5.2. lists Running Quality Index results and UTS values.

For low UTS values, the Running Quality Index values are high and for higher UTS values, the Running Quality Index values are low.

Figure 5.9. Running Quality Index Results for Sample 1
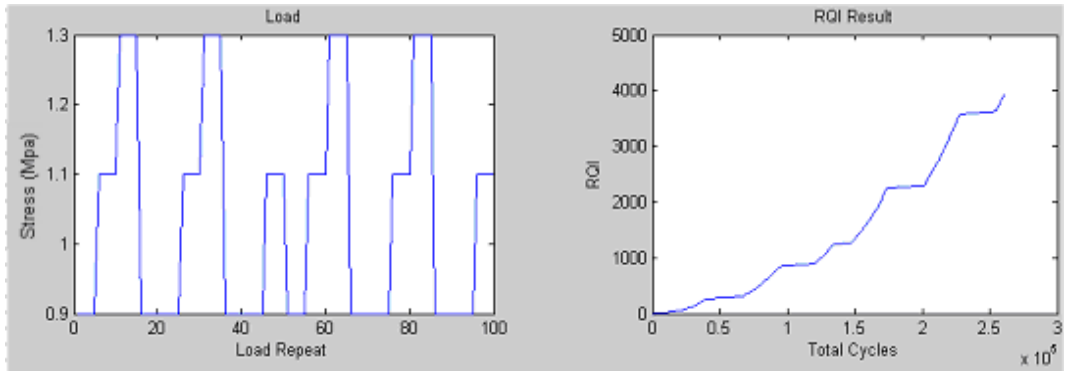
Figure 5.10. Running Quality Index Results for Sample 2
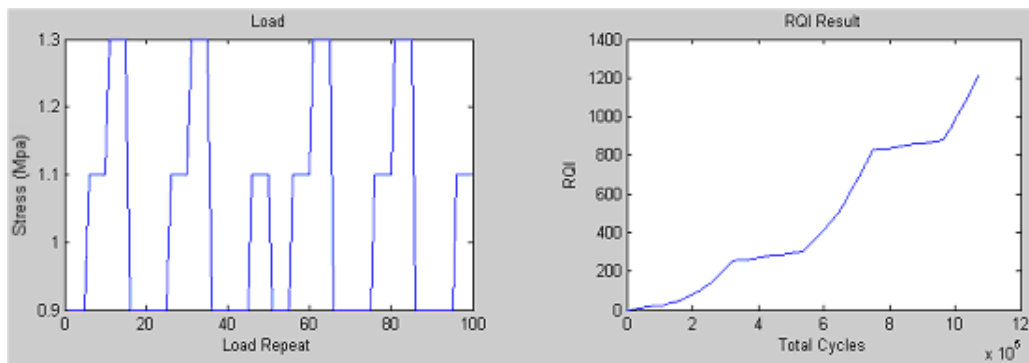
Figure 5.11. Running Quality Index Results for Sample 3
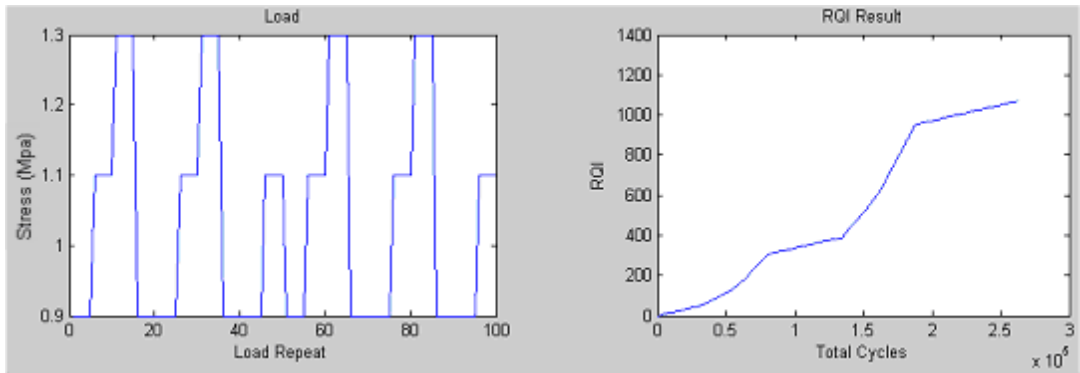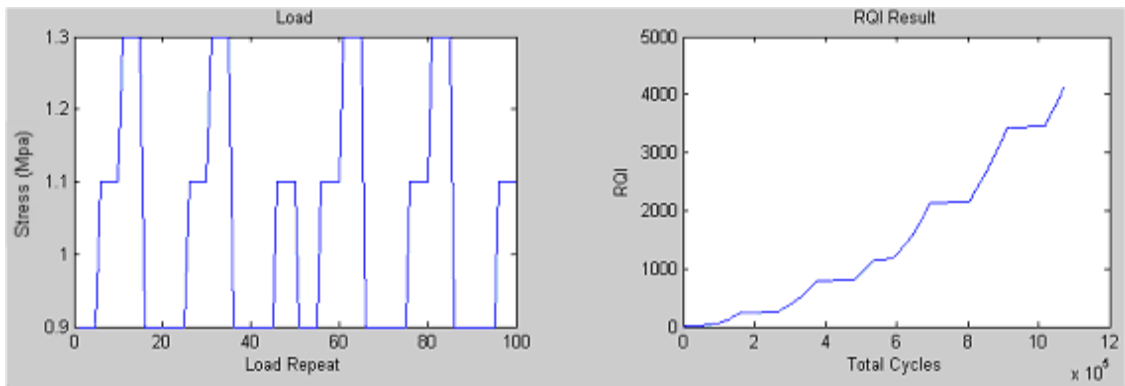
Figure 5.12. Running Quality Index Results for Sample 4
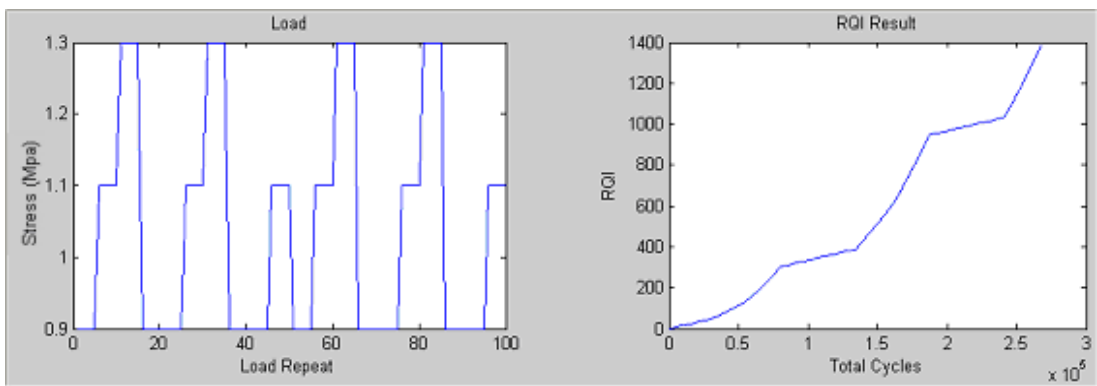
Figure 5.13. Running Quality Index Results for Sample 5
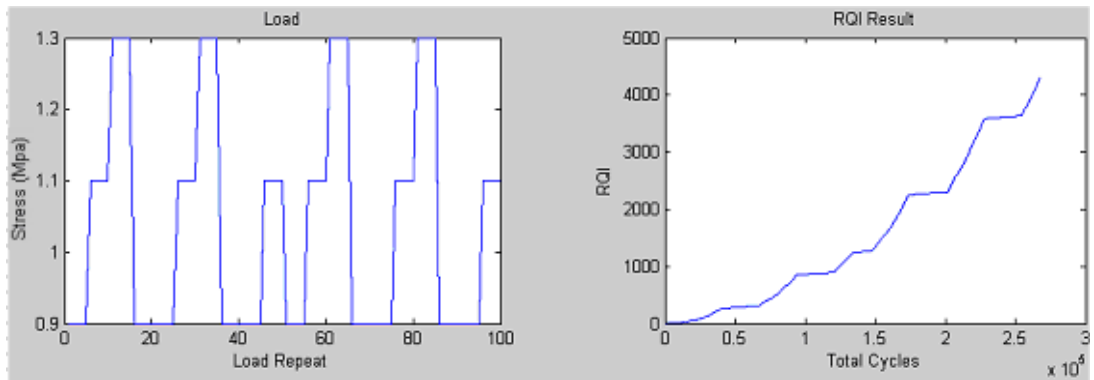
Figure 5.14. Running Quality Index Results for Sample 6
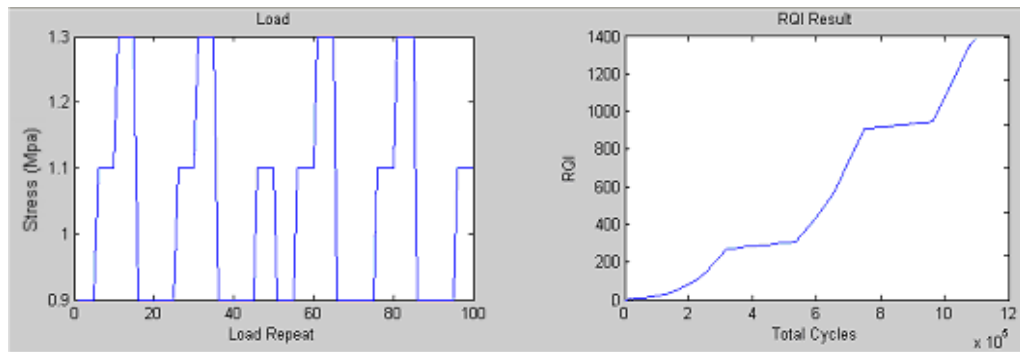
Figure 5.15. Running Quality Index Results for Sample 7
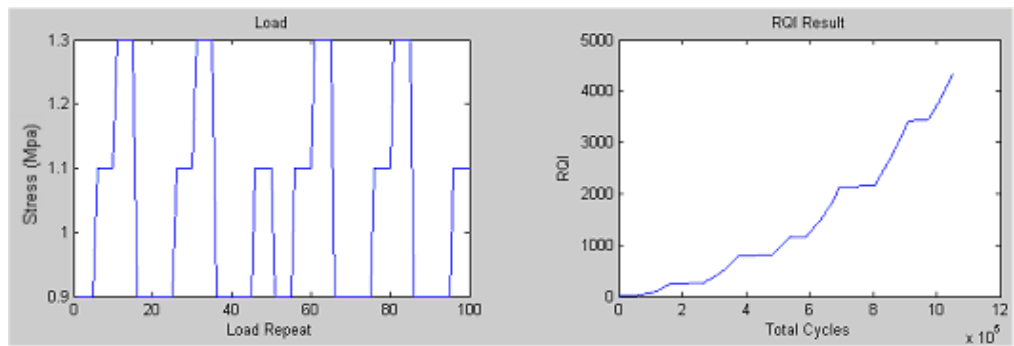
Figure 5.16. Running Quality Index Results for Sample 8

Table 5.2. Running Quality Index Results

Specimen No:	Total Cycle	Number of Repeated Loading	Temperature Treatment	RQI Result	UTS Values after experimental conditions(Newton/mm^2)
1	268020	50	25^0C	1145.9	610.09
2	268020	100	25^0C	4127.7	603.02
3	1072080	50	25^0C	1215.7	606.25
4	1072080	100	25^0C	4135.6	601.86
5	268020	50	800^0C	1388.9	455.46
6	268020	100	800^0C	4320.6	421.59
7	1072080	50	800^0C	1393.3	436.31
8	1072080	100	800^0C	4413.6	416.82

5.3. Analysis of the Results

Steel has a relatively high tensile strength compared to other materials. In this thesis a steel type was chosen for steel is being the most widely used material in machine industry: most of the components are made of steel (Martin and Iaian 2006). In many applications, the UTS is selected as the design criteria and it is a mechanical property easy to determine as compared with yield strength which requires sophisticated strain measurements. The initial region of the stress-strain curve is affected greatly by the test machine extension and therefore the stress-strain relation becomes usually nonlinear in the initial region of the stress-strain curve unless an auxiliary displacement measuring system is used.

Samples heat-treated at 800^0C for 30 minutes had lower UTS values than the samples with the no heat treatment although they were tested at the same number of cycles and the same number of repeated loading. Consider specimen 1 and 5, except the heat-treatment the test conditions are the same for these specimens. The heat treatment process resulted in a reduction in UTS value hence an increase in Running Quality Index value. The Running Quality Index is 1145.91 for specimen while it increases to 1388.9 for specimen 5. This is important since in the industrial machine usage the temperature may easily change with several factors such reduction in lubrication conditions, excessive running of the components and unexpected frictional forces. It should be noted that the temperature effect may also be included into the analysis by simply testing the specimens at different temperatures. This will be considered in future studies.

The total number of cycles is also effective in RQI as heat-treatment. Increasing number of cycles decreases UTS and hence increases RQI. This effect is related to fatigue. When a motion is repeated, the object that is doing work becomes weaker. Specimen 2 and 4 were tested at 268020 and 1072080 number of cycles, respectively. The UTS value is lower for specimen 4, reflected as the effect of number cycles. The crack length is related to total cycle; so, RQI should be a strongly function of total number of cycles.

The Running Quality Index is also capable of taking into account repeated forces. When a force is repeated it has an effect on material even it is not very big. Running Quality Index takes normal loadings (loading which are below critical level)

also as a potential risk factor, because every little effect has an important role in developing a bigger effect. Running Quality Index also takes into account the forces which are more than critical level also and it gives more risk penalty points for these forces. It counts these overloads with a counter which is included in its code and it gives more penalty points for the second, third, etc. overloads. As shown in Figures 5.13.-5.20. Running Quality Index does not always linearly increase. Sometimes it increases more, some times less. This is because of the overloads. For example the only difference between sample 1 and 2 is the force repeat levels. Sample 1 was loaded 50 times and sample 2 was loaded 100 times. The UTS is 610.09 MPa sample 1 and 603.02 MPa for sample 2. The reduction in UTS increases Running Quality Index value for sample 2. Running Quality Index also indicates more risk density in samples exposed to more repeated forces.

CHAPTER 6

CONCLUSION

In designing stage of a product, the Running Quality Index can be used to make predictions. While the designer is designing the part, the environmental conditions and the way to use the product can be simulated. The Running Quality Index could help the designer to imagine several life scenarios of the product. With such information, the designer could estimate the maximum risk number with respect to Running Quality Index and variables, and therefore decide when the product is out of use by knowing the risk number. This number could be given to the customer at purchasing and for example the maximum number could be indicated on product (example: Risk=x Risk max=xx). Running Quality Index can help customer to decide to repair or reuse the component/or part. It also helps the manufacturer to decide about remanufacturing or reuse.

In this study, a new index for the failure risk of mechanical components after the customer usage was developed. The coding of Running Quality Index was performed in MATLAB program. The index summarizes all performance history of component/or part into a single number. It is characterizing the health of the product. A shaft test rig was designed to simulate force and number of cycle effects on the quality index. Tensile tests were conducted on St-37 steel samples exposed to varying forces, number of cycles and heat treatment to calculate Running Quality Index. The experimental results showed that increasing total number of cycles or repeated forces decreased the remaining life of samples. The developed quality index resulted in more risk penalty points for increasing number of cycles and repeated forces. The Running Quality Index was also capable of defining abuse and normal use.

Online monitoring of Running Quality Index results can further save lives. Manufacturer can shut down the component/or product immediately before catastrophic failure occurs, warn the user to repair the product at the service after a certain period of time. This index can also be important for customers of second handed products because when knowing about product life and risk factors, customer can decide more clearly. The Running Quality Index developed is still in its infancy but promising. It can be adapted to any product including cars, airplanes and products of other sectors.

REFERENCES

A. Rama Chandra Murthy, G. S. Palani and Nagesh R 2005. *An Improved Wheeler Model for Remaining Life Prediction of Cracked Plate Panels Under Tensile-Compressive Overloading*. Scientist Structural Engineering Research Centre(1:203-213)

A. Murthy and G.S. Palani 2003. *Review of Fatigue Crack Growth Analysis Under Variable Loading*. Scientist Structural Engineering Research Centre (1:118-120)

About auto repair.2007. http://z.about.com/d/autorepair (accessed: July 1, 2007)

Ashby and Jones. 1998. Fatigue and Fracture Lecture Notes.

Asok Ray and Ravindra Patankar 1999. *Fatigue Growth Model Under Variable-Amplitude Loading Part:1*. Applied Mathematical Modelling.(25:980-984)

B. Kang and C. A. Tan 2000. *Parametric Instability of a Leipholz Column Under Periodic Excitation*. Journal of Sound and Vibration. (229:1097-1113)

B. Kunkler, O Duber , P. Koster, U. Krupp, C. P. Fritzen and H. J. Christ 2008. *Modelling of Short Crack Propagation*. Engineering Fracture Mechanics. (75:715-725)

B. Zafosnik, S. Glodez, M. Ulbin and J. Flasker 2007. *A Fracture Mechanics Model for the Analysis of Micro -pitting in Regard to Lubricated Rolling -Sliding Contact Problems*. International Journal of Fatigue.

D. L. Henry 1954. *A Theory of Fatigue Damage Accumulation In Steel.* Trans Asme (77: 640-655)

Edinburg Kohen 1999. *S-N Fatigue Properties* (Cambridge University Lecture Notes)

E. E. Gdoutos 2005. *Fracture Mechanics: An Introduction*. Netherlands:Springer Books

Emerging Technologies for Design Solutions. 2008. http://europe.elecdesign.com/Files/33/10777/ (accessed : January 8, 2008)

Ferinand P.Beer and E. Russell Johnston Jr. 2003. *Cisimlerin Mukavemeti.* Türkiye:Beta Yayınevi.

Griffith.1924 *The Theory of Rupture.* International Congress for Applied Mechanics.

Griffith 1921. *The Phenomena of Rupture and Flow in Solids.* The Royal Society of London 1921.

Heinz P. Bloch and Fred K. 2006. *Machinery Uptime Volume 5*. New York : Elsevier Books.

Haris H. 1976. *Strategy of Experimentation*. Dupont Short Course Notes.

Hoang Pham 2006. *Handbook of Engineering Statistics*. Netherlands:Springer Books.

K. L. Mills, Xiaoyue Zhu, Schuichi Takayama and M. D. Thouless 1996. *The Mechanical Properties of a Surface - Modified Layer on Dimethylsiloxane.* Department of Mechanical Engineering University of Michigan, USA

L. Franke and G. Dierkes 1999. *A Non-Linear Fatigue Damage Rule with an Exponent Based On a Crack Growth Boundary Condition*. International Journal of Fatigue. (21:761-764)

L. M. Jadaan and Gyekenyesi J. P. 1996. *Creep Life of Ceramic Components Using a Finite Element Based Integrated Design Program*. Journal of Engineering for Gas Turbines and Power.(120:162-171)

L. Toth and P. Rossimanith 2003. *Historical Background and Development of Charpy Test*. Vienna University of Technology Lecture Notes

Laura Ceriolo and Angelo Di Tomasso 1998. *Fracture Mechanics of Brittle Materials.* Symposium in Civil Engineering. (1:2-18)

Levon Çapan 2003. *Metallere Plastik ekil Verme*. Türkiye:Ça layan Yayınevi

Lucie Vandewalle 2005. *Building Material Lecture Notes*

M. Fonte, F. Romeiro and M. Freitas 2007. *Environmental Effects and Surface Roughness on Fatigue Crack Growth at Negative R-Ratios.* International Journal of Fatigue.(29:1971-1977)

Madhamarao Krishnadev and Maude Larouche 2008. *Fracture of High Carbon High Strength Anchor Rods.* Engineering Failure Analysis.(15:1009-1018)

Mathnstuff . 2007. http://www.mathnstuff.com/math/spoken/ (accessed : October 10, 2007)

Mehmet Emin Yurci 1992. *Tala sız ekil Verme.* Türkiye : Yıldız Teknik Üniversitesi Matbaası

Milan Jirasek and Peter Grassl 2007. *Evaluation of Directional Mesh Bias in Concrete Fracture Simulations Using Continuum Damage Models.* Engineering Fracture Mechanics.(54:263-300)

Neil Wahl 2001. *Spectrum Fatigue Lifetime and Residual Strength for Fiberglass Laminates in Tension.* The American Institute of Aeronautics and Astronautics

S. E. Stanzl H. Mayer 2001. *Fatigue and Fatigue Crack Growth of Aluminum Alloys at Very High Numbers of Cycles.* International Journal of Fatigue (23:263-300)

S. M. Marco and W. L. Starkey 1954. *A Concept of Fatigue Damage.* Trans Asme (76: 627-632)

S. S. Manson and J. C. Freche 1966. *Application of A Double Linear Damage Rule to Cumulative Fatigue.* NASA Publications 1966.

Sinan Köksal 2005. *Fracture Mechanics Lecture Note.* Celal Bayar Üniversitesi Makine Mühendisli i Bölümü Ders Notları

Shawn M. Kelly 2005. *Crack Initiation and Propagation.* Laboratory of Scientific Visual Analysis Work Notes.

R. D. McCammon and H. M. Rosenberg 2000. *The Fatigue and Ultimate Tensile Strength of Metals.* London:Royal Society of London

R. Desmorat, F. Ragueneau and H. Pham 2006. *Continuum Damage Mechanics for Hysteresis and Fatigue of Quasi - Brittle Materials and Structures.* Engineering Fracture Mechanics.

R. H. J. Peerlings and W. A. M. Brekelmans 2006. *Continuum Damage Approach to Fatigue.(*Eindhoven : University of Technology Press)

R. R. Gatts 1961. *Application of A Cumulative Damage Concept To Fatigue.* Asme Journal of Basic Engineering.

R. R. Gatts 1962. *Cumulative Fatigue Damage with Random Loading.* Trans Asme Journal of Basic Engineering (84:403-409)

Rodrigue Desmorat 2000. *Damage and Fatigue CDM Modelling for Fatigue of Materials and Structures.* Revue Europeenne De Genie Civil.(10:849-877)

Terry Engelder and Mark P. 1995. *Loading Configurations and Driving Mechanisms for Joints Based on the Griffith Energy Balance Concept.* Tectonophysics. (256:253-277)

Thomas P. Ryan 2006. *Modern Experimental Design.* London:Wiley Series

Tom Martin and Iaian A. 2006. *The Tay Rail Bridge Disaster Revisited.* Proceedings of the Institution of Civil Engineers.

W. W. Gerberich 1998. *Low and High Cycle Fatigue-A Continuum Supported By AFM Observations.* Pergamon(46:5007-5021)

Walter Schlitz 1996. *A History of Fatigu*e. Engineering Fracture Mechanics.(54:263-300)

World Nuclear Association. 2007. http://www.world-nuclear.org/images (accessed : May 4, 2007)

Xiaoting Liang and William L. Headrick 2006. *CDM Modelling of the Failure of Refractory Cup Under Thermal Loading.* Refractory Applications and News.(11:17-23)

Xu Chena, Dan Jina and Kwang Soo Kim 2005. *Fatigue Life Prediction of Type 304 Stainless Steel Under Sequential Biaxial Loading.* International Journal of Fatigue. (28:289-299)

Yung-Li Lee, Jwo Pen, Richard Hathaway and Mark Barkey 2005. *Fatigue Testing and Analysis Theory and Practice*. Tokyo:Elsevier Books